Revision 2

On Silica-Rich Granitoids and their eruptive equivalents

Carol D. Frost[1], B. Ronald Frost[1], James S. Beard[2]

[1]Department of Geology and Geophysics, University of Wyoming, Laramie WY 82071 USA

[2]Virginia Museum of Natural History, 21 Starling Ave., Martinsville VA 24112 USA

Abstract

Silica-rich granites and rhyolites are components of igneous rock suites found in many tectonic environments, both continental and oceanic. Silica-rich magmas may arise by a range of processes including partial melting, magma mixing, melt extraction from a crystal mush, and fractional crystallization. These processes may result in rocks dominated by quartz and feldspars. Even though their mineralogies are similar, silica-rich rocks retain in their major and trace element geochemical compositions evidence of their petrogenesis. In this paper we examine silica-rich rocks from a variety of tectonic settings, and from their geochemical compositions identify six groups with distinct origins. Three groups form by differentiation: *ferroan alkali-calcic* magmas arise by differentiation of tholeiite, *magnesian calc-alkalic or calcic* magmas form by differentiation of high-Al basalt or andesite, and *ferroan peralkaline* magmas derive from transitional or alkali basalt. *Peraluminous leucogranites* form by partial melting of pelitic rocks, and *ferroan calc-alkalic* rocks by partial melting of tonalite or granodiorite. The final group, the *trondhjemites*, is derived from basaltic rocks. Trondhjemites include Archean trondhjemites, peraluminous trondhjemites, and oceanic plagiogranites, each with distinct geochemical signatures reflecting their different origins. Volcanic and plutonic silica-rich rocks rarely are exposed together in a single magmatic center.

Therefore, in relating extrusive complements to intrusive silica-rich rocks and determining whether they are geochemically identical, it is important to compare rocks formed from the same source rocks by the same process; this classification aids in that undertaking.

Keywords: granite, rhyolite, geochemistry, trondhjemite, leucogranite, petrogenesis

Introduction

Silica-rich granites and rhyolites are components of igneous rock suites found in many tectonic environments, including convergent margins, divergent margins, and intraplate hotspot and extensional regimes. They are most voluminous in continental settings but also occur in oceanic environments. Silica-rich magmas may arise from a variety of processes including partial melting, fractional crystallization, magma mixing, and extraction of melt from a crystal mush. Although all are dominated by quartz and feldspars, silica-rich rocks form by different petrogenetic processes and from various parental materials, and they retain in their major and trace element geochemical compositions evidence of their petrogenesis. In this paper we identify six geochemically distinct groups of high-silica granitic rocks and rhyolites that appear to have formed by nearly end-member processes of partial melting or differentiation (either fractional crystallization or melt extraction). We suggest that recognition of these groups is a necessary preliminary to resolving questions about high-silica rocks, including for example, the relationship of volcanic rocks to their plutonic complements.

Using a similar geochemical approach, Frost et al. (2001) recognized peraluminous leucogranites as a special family of granitoids. These rocks are characterized by high silica (>70%) and range from ferroan to magnesian and from calcic to alkalic. Their only common geochemical features are their high silica content and peraluminous nature. Because all of the leucogranite suites tabulated in their study contained rocks with more than 70% SiO_2 (see Figure 3 in Frost et al., 2001) they put the cut-off for peraluminous leucogranites at 70% SiO_2. In addition to peraluminous leucogranites there are several other groups of silica-rich granitoids, many of which are true leucogranites, and all of which are summarized in this paper.

Our approach relies first on major element analyses utilizing four geochemical indices: Fe-index, modified alkali-lime index (MALI), alumina saturation index (ASI), and alkalinity index (AI) (Frost et al., 2001; Frost and Frost, 2008; Table 1). As silica content increases in granitoids, the proportions of other elements necessarily decrease, and as a result, the oxides used in these geochemical indices (e.g. Al_2O_3, CaO, Na_2O, K_2O, FeO^{tot}, and MgO) make up an increasingly small proportion of the total. Nevertheless, different occurrences of silica-rich rocks define distinct characteristics, ferroan and magnesian, alkali to calcic, and metaluminous, peraluminous, and peralkaline. Because trace element contents of silica-rich rock suites vary more than do the major element oxides we supplement the major element geochemical indices with consideration of minor and trace element variations. We then consider how our recognition of these six groups contributes to solving several petrologic problems surrounding the origin of silica-rich granite and rhyolite.

Definition of silica-rich granite and rhyolite

Before classifying silica-rich granitoids, we must settle questions about terminology. One term applied to silica-rich rocks, leucogranite, is defined from modal mineralogy: leucogranites are granites in which the volume of mafic minerals is less than 5%. Because modal mineralogy is not regularly reported for all rocks for which geochemical analyses are obtained, it would be convenient to approximate modal abundance of mafic minerals with a geochemical parameter. One possibility is to use the ferromagnesian oxides (i.e. the sum of oxides that make the ferromagnesian minerals, TiO_2, Fe_2O_3, FeO, MnO, and MgO). We evaluate this possibility using seven granitoid suites for which both modal and chemical analyses have been published (Fig.1a). This compilation includes analyses for the ferroan alkali-calcic Topsails batholith (Whalen and Currie, 1984), the magnesian calcic metaluminous Klamath granitoids (Holz, 1971), the calcic peraluminous Cornucopia stock (Johnson et al., 1997), the calc-alkalic metaluminous Tuolumne intrusion (Bateman and Chappell, 1979) and Palisade Crest pluton (Sawka et al., 1990), and the alkali-calcic metaluminous Ballachulish pluton (Weiss and Troll, 1989). As shown in Figure 1a, rocks with a color index (defined as the volume % of mafic minerals) of 5% equate to a sum of ferromagnesian oxides that varies from 2 to 4%. A variation of 2% is large considering that silica-rich granitoids are composed mainly of quartz and feldspars, and hence are dominated by SiO_2, Al_2O_3, CaO, Na_2O and K_2O. The variation is explained by recalling that these oxides can be incorporated in a variety of minerals including Fe-Ti oxides, biotite, hornblende, and pyroxenes, minerals that have a wide range in molar volumes. A rock containing biotite and hornblende, both of which also incorporate feldspar components, will have a higher

color index than a rock of the same composition that contains pyroxenes or only Fe-Ti oxides.

Another possibility is to identify a specific SiO_2 content above which granitic rocks have no more than 5% mafic minerals. We evaluate this possibility in Figure 1b, which plots color index of these suites against silica. Approximately 52% of the granites from this data set that contain more than 70% silica have color index < 5 and hence are true leucogranites. However, the other 48% have color index > 5 and, hence must be considered regular granites. We conclude that it is not possible to determine precisely from the relative abundances of the oxides that produce ferromagnesian minerals whether a given rock is a true leucogranite. Because the term leucogranite should be assigned based on modal mineralogy and there is no satisfactory geochemical proxy, in this paper we will characterize igneous rocks that have more than 70% silica as *silica-rich*. We have chosen this silica content to be consistent with the classification of peraluminous leucogranites (Frost et al. 2001), and because other authors have adopted silica contents of $\geq$70% to denote high-silica granites (e.g., Lee and Morton, 2015). The silica-rich intrusive rocks we discuss include granitic rocks with varying proportions of alkali-feldspar and plagioclase, from alkali-feldspar granite to trondhjemite. In referring to these collectively as silica-rich granites, we use the term granite *sensu lato*.

Issues of terminology also affect the literature on high-silica eruptive rocks. Petrologically the distinction between dacite and rhyolite is clear – dacite has phenocrysts of plagioclase and quartz whereas rhyolite has phenocrysts of alkali feldspar and quartz. Many siliceous eruptive rocks lack phenocrysts and petrologists must classify them by their geochemistry. Unfortunately, the geochemical classification of Le Bas et al. (1986)

does not distinguish between Na_2O and K_2O. As a result, an aphyric eruptive rock with 75% SiO_2, 2% Na_2O, and little to no K_2O is classified as rhyolite, even if the solidified magma is a trondhjemite with no K-feldspar. In parallel with the classification of plutonic rocks, such low-potassium rhyolites technically should be classified as dacites. Nevertheless, in this paper we will follow Le Bas et al. (1986) and refer to the eruptive equivalents of silica-rich granites as rhyolites with the realization that some rhyolites (for example, of Fiji) contain less than 2% K_2O and are the eruptive equivalent of trondhjemite, not granite *sensu stricto*.

Approach

Silica-rich granitoids and associated rhyolites may form by one of two broad petrogenetic processes: partial melting and differentiation. The process of differention is likely to involve extreme fractional crystallization, but other processes, such as magma mixing and melt extraction from a crystal mush may also be involved. Taking into account the range of compositions of the sources that have partially melted or differentiated, it is possible to recognize six groups of silica-rich rocks that form by distinct magmatic processes (Table 2). These groups are identified primarily based upon their major element composition, as indicated by Fe-index, modified alkali-lime index, alumina saturation index, and alkalinity index (Frost et al., 2001; Frost & Frost, 2008; Table 1). The Fe-index distinguishes rock suites that have undergone iron-enrichment, either by fractionation or during partial melting at relatively reducing conditions. Because this index relies on the abundances of FeO^{tot} and MgO, both of which compose a relatively small percentage of the sum of major element oxides, for high-silica rocks it is

139 important to take into consideration the possible effect of analytical uncertainty on the
140 resulting values for Fe-index.

141 The modified alkali-lime index (MALI), a modification of the alkali-lime index of
142 Peacock (1931), is a robust discriminator for silica-rich granitic rocks in which CaO,
143 Na_2O and K_2O are major constituents (Frost et al., 2008). It distinguishes rocks
144 dominated by calcic to intermediate plagioclase from those with more sodic plagioclase
145 and potassium feldspar. However, it does not separate sodium-rich rocks from potassic
146 ones, a limitation that masks distinctions in some groups of granitoids as we discuss
147 below.

148 Two other indices refer to the relative abundances of molecular Al compared to
149 calcium, sodium, and potassium (the aluminum saturation index, ASI) and the abundance
150 of Al relative to alkalis (the alkalinity index, AI). ASI was defined by Shand (1927) and
151 modified by Zen (1986) as the ratio Al/(Ca – 1.67P + Na + K). Rocks with ASI >1 are
152 peraluminous rocks (they contain more Al than can be accommodated in feldspars alone).
153 Rocks with ASI <1 and molecular Na + K < Al are metaluminous (that is, they have
154 excess Ca after aluminum has been accommodated in feldspars). The alkalinity index was
155 defined by Shand (1927) as Al – (K + Na). Rocks with AI > 0.0 are metaluminous (or
156 peraluminous), whereas those with AI < 0.0 are peralkaline.

157 In this paper we also utilize various trace elements (Rb, Sr, Zr, Y, Nb) and rare
158 earth elements (REEs) that have been used to gain insights into petrologic processes
159 (Watson and Harrison, 1983; Pearce et al., 1984; Halliday et al., 1991; Moyen, 2009).
160 Unlike basaltic rocks where trace elements record melting or crystallization of major
161 rock-forming minerals, in granitic rocks many trace elements, such as Zr, Y, Nb and the

REEs, are present as major constituents in trace phases (Bea, 1996). This means that in addition to providing information on the magma sources for high-silica granitoids, trace element compositions also may provide important information about both major and minor phases that were differentiating or that were residual during the formation of silica-rich rocks.

Results

Six Classes of Silica-rich Granitoids

We recognize six groups of silica-rich rocks: 1) strongly peraluminous rocks (i.e., peraluminous leucogranites of Frost et al., 2001), 2) ferroan calc-alkalic rocks, 3) trondhjemites (i.e., sodic magnesian calcic rocks), 4) ferroan alkali-calcic rocks, 5) magnesian calc-alkalic to calcic rocks, and 6) peralkaline rocks (Table 2). Below we describe the geochemical characteristics of these groups and the type examples of intrusive and extrusive rocks that illustrate each.

1. Peraluminous leucogranite and rhyolite. Peraluminous leucogranites and rhyolites are distinguished by their high ASI, with values that may extend to 1.5, and their wide range in Fe-index and MALI (Frost et al., 2001). We chose the Miocene Makalu granite from the Himalayas (Visona and Lombardo, 2002) and Miocene-Pliocene Macusani rhyolite from Peru (Pichavant et al., 1988ab) as intrusive and extrusive examples of this rock type. These suites are composed of tourmaline and two-mica granites and volcanic rocks that are strongly peraluminous. They likely originated from a metapelitic source rock by dehydration melting of muscovite followed by incipient dehydration melting of biotite (Pichavant et al., 1988b, Visona and Lombard, 2002).

These rock suites are alkali-calcic and cover a much narrower span in MALI content than the Harney Peak peraluminous leucogranites of Frost et al. (2001) (Figure 2). This reflects the derivation of large peraluminous batholiths like Harney Peak from multiple batches of magmas that were generated from different sources under different conditions of melting (Nabelek et al., 1992) in contrast to the rather simple melting relations of the Makalu granite and Macusani rhyolite. Most samples are ferroan, although the Mascusani suite includes five much more magnesian samples (Figure 2ad). Patiño Douce and Harris (1998) showed that dehydration melting of metapelitic rocks at 6-8 kb produced melts that are virtually identical to Himalayan peraluminous leucogranites. The Fe-index of the melts decreases with increased degree of partial melting (Patiño Douce and Harris, 1998).

2. Ferroan calc-alkalic granite and rhyolite. Ferroan calc-alkalic granites are widespread, composing, for example, most of the 1.4 Ga "anorogenic" or "A-type" granites of the southwestern United States. The type example of ferroan calc-alkalic granite described by Frost and Frost (2011) are the ~1.88 Ga granites from Carajas, Brazil, which we refer to as Amazonia granites. They are distinctive in that, unlike other ferroan granites described by Frost and Frost (2011), they are restricted to relatively high-silica compositions. Silica contents greater than 70% are common, and these rocks commonly span the metaluminous-peraluminous boundary. These biotite ± hornblende granites are interpreted to form by melting of quartzofeldspathic crust (Dall'Agnol and Oliveira, 2007; Oliveira et al., 2009), a conclusion supported by experimental work (Skjerlie and Johnston, 1993; Patiño Douce, 1997). Our type example of an extrusive ferroan calc-alkalic suite is the 27 Ma Coyote Summit rhyolite tuff member of the

Shingle Pass Formation from the central Nevada ignimbrite field (Best et al., 2013). These tuffs are calc-alkalic, and, with one exception, ferroan. Like the Amazonian granites, the tuffs range from metaluminous to peraluminous. Silica contents are uniformly high, 73.2-76.1% SiO_2.

3. Trondhjemite (magnesian calcic granite and rhyolite). Trondhjemites, leucocratic tonalites dominated by quartz and plagioclase, are uniformly calcic and typically magnesian. They are important components of Archean gneiss terrains, and are a constituent of oceanic arc and ophiolite rock assemblages. The extrusive equivalents, occasionally called quartz keratophyres, are associated with mafic volcanic rocks in oceanic settings. For our type examples of magnesian calcic silica-rich rocks we have chosen the 12 Ma Wainivalau trondhjemite pluton and the 7 Ma Udu high-silica volcanic rocks, both from Fiji (Stork, 1984). Silicic rocks are uncommonly abundant in Fiji compared to most intra-oceanic arcs; these formed during the transition from arc to back-arc basin (Gill et al., 1984). The silicic volcanic rocks (72-78% SiO_2) are characterized by low K and high Na/Ca, and are strongly calcic. The plutonic rocks extend to lower SiO_2 contents, but likewise plot in the calcic field (Figure 2be). The plutonic rocks are magnesian and mainly metaluminous, whereas the volcanic rocks span the ferroan/magnesian and metaluminous/peraluminous fields.

There are some important the distinctions between oceanic trondhjemites such as those from Fiji and other trondhjemites, including those in Archean gneiss terrains and peraluminous trondhjemites in continental settings. We consider the processes responsible for these different groups of trondhjemites at greater length in the discussion.

4. Ferroan alkali-calcic granite and rhyolite. Many ferroan, alkali-calcic silica-rich granites are part of suites that encompass a range in silica content, such as the Sherman batholith of Wyoming, although other ferroan granitoids, such as the Finnish rapakivi granites, occur as large intrusions that are not associated with mafic rocks (Frost and Frost, 2011). These rocks, also known as "A-type granites", are distinguished by their high Fe index and their alkali-calcic composition and may be either metaluminous or slightly peraluminous (Frost and Frost, 2011; Fig. 3). Ferroan alkali-calcic granites and rhyolites are generally more iron-enriched, more alkalic, and less peraluminous than the ferroan calc-alkalic peraluminous granites (Fig. 3).

Our type example for a silica-rich granite in this family is the Nebo granite, an extensive ferroan granite that caps the ~2 Ga Bushveld complex of South Africa. Our dataset comes from a portion of Nebo granite in the eastern Bushveld Complex studied by both Kleeman and Twist (1989) and Hill et al. (1996). These rocks are strongly ferroan, alkali-calcic and metaluminous to slightly peraluminous (Fig. 3). Mathez et al. (2013) call on fractional crystallization of Bushveld mafic liquids to form the ferroan felsic rocks of the complex, a hypothesis that is consistent with geochemical and isotopic data, as well as with known age relations. The type rhyolites are the Yellowstone Plateau rhyolites, 2.2 Ma and younger, including both those that tapped the main subcaldera magma reservoir and extra-caldera lavas (Hildreth et al., 1991). The rhyolites have high silica contents (74.6 - 77.1%, plus one sample with 70.8% SiO_2). The rocks with the highest silica span the alkali-calcic to calc-alkalic boundary. All samples record Fe-index of 0.9 or higher, and range from metaluminous to peraluminous. Hildreth et al. (1991) called on partial melting of Quaternary mantle-derived basaltic crust to produce

255 the silicic magmas at Yellowstone, although similar fayalite rhyolites in the Eastern
256 Snake River Plain are interpreted to represent extreme differentiation of tholeiitic basalt
257 (McCurry et al., 2008).
258
259 **5. Magnesian calc-alkalic to calcic granite and rhyolite.** Magnesian calc-alkalic
260 granites and rhyolites are commonly associated with continental arc batholiths and
261 volcanoes, where the silica-rich rocks are less abundant than the basaltic, andesitic, and
262 dacitic members of the suite. In addition to being magnesian and calc-alkalic, these
263 suites are overwhelmingly metaluminous. However, the most silica-rich members of the
264 suites can include peraluminous rocks and some may be ferroan (See Frost et al., 2001,
265 Fig. 4).
266 Our example of this type of high-silica granite is the leucogranite associated with
267 the Half Dome granodiorite of the Late Cretaceous Tuolumne intrusive series in the
268 Sierra Nevada batholith, California (Coleman et al., 2012). The Half Dome granodiorite
269 consists of multiple km-scale sheets that range from mafic granodiorite in the west to
270 leucogranite in the east. Coleman et al. (2012) interpret the leucogranites to have formed
271 from late-stage silica-rich melts that separated from a crystal mush and migrated through
272 each sheet to accumulate near the top of the magma system.
273 The corresponding type magnesian, calc-alkalic rhyolite is the Quaternary rhyolite
274 of the South Sister volcano in Oregon (Brophy and Dreher, 2000; Fierstein et al., 2011).
275 The 50 to 2 ka South Sister lavas are andesite, dacite, and rhyolite. Rhyolites erupted
276 throughout the history of the volcano and both peripherally and centrally; they are calc-
277 alkalic and mainly magnesian, although the most siliceous samples are ferroan. South

Sister rhyolites with SiO_2 > 70% are weakly peraluminous. The authors studying these suites propose that the diverse magma compositions are related by differentiation, and that the rhyolites formed by extraction of fractionated liquid from crystal-rich reservoirs (Brophy and Dreher, 2000; Fierstein et al., 2011; Stelten and Cooper, 2012).

6. Peralkaline granite and rhyolite. Peralkaline granites and rhyolites typically occur with alkali basalts in a bimodal association where intermediate rocks are absent. They are most commonly found in continental intraplate settings affected by rifting, although the association is also present on some oceanic islands, and more rarely in orogenic settings. Our example of peralkaline granite is Brandberg (Schmitt et al., 2000) and peralkaline rhyolite is Pantelleria (Avanzinelli et al., 2004, White et al., 2009).

The Brandberg massif of northwestern Namibia formed between 133 and 130 Ma, contemporaneously with the flood basalts and associated felsic volcanism of the Etendeka-Paraná province. The ~23 km diameter intrusive complex is composed mainly of hornblende-biotite granite (Schmitt et al., 2000). In the southwestern part of the intrusion, peralkaline granite sills and dikes of the Amis intrusion cut the main granite massif. Schmitt et al. (2000) call on fractionation of a common tholeiitic basalt parent to form both granites. They suggest that extreme degrees of fractionation alone produce the peralkaline granites, whereas the hornblende-biotite granite experienced substantial crustal assimilation.

Avanzinelli et al. (2004) used geochemical data and clinopyroxene crystal chemistry of mafic and felsic lavas and pyroclastic rocks from Late Pleistocene Pantelleria Volcano, Italy to determine the origin of the peralkaline, type-locality pantellerites. In their model, parental alkali basalts differentiated at depth to form

gabbroic rocks. Subsequent partial melting of these gabbroic rocks produced a trachytic magma that differentiated to form the peralkaline suite.

Trace Element Characteristics of Silica-rich Granitoids

Rb and Sr. Rb and Sr are two trace elements that can be used to monitor fractional crystallization or melting (Halliday et al., 1991), which as suggested above, are processes that can produce silica-rich granitoids. Sr is compatible in plagioclase, with $D_{Sr}^{plag-melt} = 1.5$ to 7. D increases with increasing albite content of the plagioclase (Korringa and Nobel, 1970; Blundy and Wood, 1991). Sr is also compatible in alkali feldspar, with $D_{Sr}^{Afs-melt} = 2$ to 5. D increases with increasing albite component in the alkali feldspar (Long, 1978). In contrast, Rb is incompatible in plagioclase, with $D_{Rb}^{plag-melt} = 0.1$ or less (Arth, 1976; Mahood and Hildreth, 1983; Nash and Crecraft; 1985) and slightly compatible to incompatible in alkali feldspar (Arth, 1976; Long, 1978; Mahood and Hildreth, 1983; Nash and Crecraft; 1985). The major hosts for Rb in igneous rocks are the micas. Biotite contains 2 to 8 times more Rb than coexisting potassium feldspar (Mahood and Hildreth, 1983; Nash and Crecraft; 1985) and 2 to 3 times more Rb than coexisting muscovite (Yang and Rivers, 2000).

The Rb and Sr abundances of the six classes of silica-rich granitoids and their related rhyolites show distinctly different patterns between those that are inferred to have formed primarily by differentiation (Fig. 4a) and those that are inferred to be crustal melts (Fig. 4b; note the different scales for Rb on Figs. 4a and 4b). The suites interpreted to form by differentiation show trends that decrease in Sr from around 300 ppm to less than 1 ppm with a concomitant increase in Rb from around 50 to up to 1100 ppm. The

only suite that lies off this trend is the leucogranite from Half Dome, which has a higher Rb at a given Sr content.

Each of the suites that are inferred to have formed by partial melting defines a field that displays a range in Sr abundance but which cluster in Rb abundance (Fig. 4b). Suites that are inferred to have formed by partial melting of pelitic rocks (Makalu and Macusani) have Rb abundances (300-600 ppm) (Fig. 4b) that are much higher than those reported for the differentiated rocks with a similar Sr content (Fig. 4a). The suites that formed by melting of tonalite or granite (Coyote Summit, Amazonia) have intermediate Rb abundances (around 200) that also are higher than the suites formed by differentiation. The suites from Fiji that are inferred for have formed by melting of basalt have very low Rb contents (less than 100 ppm) that are lower than suites formed by differentiation.

Trace-element modeling using bulk $D_{Rb} = 0.1$ and bulk $D_{Sr} = 2$ (Halliday et al., 1991) shows that the suites that are inferred to have formed by fractional crystallization lie along a trend defined by Rayleigh fractionation of an alkali basalt (lower solid line on Fig. 4c). Although extreme fractionation of alkali basalt could have produced the peralkaline rocks of Brandberg (Schmidt et al., 2000), alkali basalt is unlike to have been the parental melt to the rhyolites of South Sister or the ferroan alkali-calcic granites or rhyolites. These suites could have been produced, however, by differentiation of a basaltic rock in which Rb has been somewhat elevated by crustal assimilation. The leucogranite from Half Dome, interpreted to form by separation of melt from crystals (Coleman et al., 2012), defines a field that overlaps the trend modeled by fractional crystallization of the Half Dome granodiorite.

Geochemical modeling shows that the Sr-poor peraluminous granites and rhyolites may have formed by partial melting of metapelite. In partial melting of pelitic rocks the major phases melting are muscovite and biotite, and, if water pressure is high enough, plagioclase (Patiño Douce and Harris, 1998). Thus the effective bulk composition of the source for melting of pelitic rocks may be distinctly richer in Sr and Rb than the bulk shale composition used in the equilibrium batch models. (Batch melting models are shown by dashed lines on Fig. 4c and d.) The more Sr-rich ferroan calc-alkalic rocks may have formed by batch melting of typical upper crust. The low Rb contents of the calcic rocks from Fiji may reflect derivation from a Rb-poor mafic source (Stork, 1984). In addition, because K and Rb are fractionated from a trondhjemitic melt into the fluid (Adam et al., 1997), evolution of a vapor phase prior to crystallization of biotite and potassium feldspar will result in depletion of Rb and K in the crystallization products of that melt (Beard, 1998).

The Rb-Sr compositions of the rocks from Fiji and Amazonia show that the origins of these suites are far more complex than simple partial melting. The extensive range in Sr contents in the plutonic rocks of Wainivalau compared to the volcanic rocks of Udu suggest that a considerable amount of cumulate plagioclase may be present in the plutonic rocks. The wide range in Sr contents from the Amazonia rocks also suggests that these rocks underwent fractional crystallization after the original melt formed.

Zr. Two main factors control the Zr content of granitic rocks – composition and temperature. Higher silica and alumina relative to alkalis support less Zr in the melt, whereas higher alkalis relative to silica and alumina will enhance Zr solubility. The

effects of temperature and composition are shown in Figure 5 as calculated by the equations of Watson and Harrison (1983). The two lines on Figure 5 represent the compositional range over which Watson and Harrison (1983) suggest their equation should be used. Figure 5 shows that over a temperature range that might be expected for rhyolites (from 700° – 900°C) and the range of compositions modeled by Watson and Harrison (1983) the Zr content of granitic melts may vary by an order of magnitude.

The Zr contents of natural rhyolites actually define a much greater range in values than calculated from the Watson and Harrison equation, because as pointed out by Watson (1979) the high Na + K in peralkaline magmas stabilize Zr in the melt, which is the reason why Watson and Harrison (1983) restrict the compositional range over which their equations can be applied. The peralkaline glasses from Pantelleria contain up to 2400 ppm Zr (Neave et al., 2012), an amount that would indicate a Zr-saturation temperature of up to 1040°C, which is well outside the temperature limits of 800°-870°C estimated for the eruption of the pantellerite magmas (Neave et al., 2012). The extreme Zr contents in some Brandberg samples probably result from both the Zr enrichment common in alkaline rocks and from accumulation of zircon in the peralkaline granite.

The variation in Zr contents for the other silica-rich granites and rhyolites fit fairly well what would be predicted from the expressions of Watson and Harrison (1983). Peraluminous rhyolites and leucogranites, which form at relatively low temperatures have the lowest Zr contents (Figure 6a,b). The Zr contents of the other type examples increasing in the order of calcic – calc-alkalic – alkalic, an order that is consistent with the observations of Watson (1979) and Watson and Harrison (1983) that increasing Na + K contents enhance the solubility of Zr in a melt.

Y and Sr/Y. As noted above, because Sr is compatible in feldspars, the Sr contents of magmas reflect the involvement of plagioclase and to a lesser extent alkali feldspar in the formation of silica-rich rocks. (A negative Eu anomaly accompanying low Sr abundances may indicate plagioclase removal or retention in the source.) Y, with behavior similar to Yb but typically having an order of magnitude higher abundance, is a proxy for heavy rare earth element (HREE) content. It is strongly partitioned into garnet and hornblende, and into accessory minerals including apatite and zircon (Pearce and Norry, 1979; Nardi et al., 2013). The Sr/Y ratio can indicate the pressure of partial melting; high pressure melting produces melts with high Sr/Y because plagioclase is unstable and releases Sr to the melt but garnet is stable and retains Y in the source. However, as pointed out by Moyen (2009), the Sr/Y of mantle and crustal sources is quite variable, and high Sr/Y does not always indicate high pressure melting: it is possible to derive a magma with high Sr/Y by melting a high Sr/Y source at low pressure.

The Sr/Y vs. Y diagram has been used to discriminate certain felsic arc volcanics ("adakites") and Archean tonalites and trondhjemites from other igneous suites (Defant and Drummond, 1990; Moyen, 1999). The former are characterized by high Sr (>300 ppm) and low Y and HREE abundances ($Y \leq 18$ ppm, $Yb \leq 1.8$ ppm; Martin, 1999); Sr abundances are lower and Y abundances higher in most other igneous rocks. Of the groups of silica-rich rocks defined in this paper, none of them lie within the high Sr/Y "adakite" field defined by Defant and Drummond (1990). At the other extreme, Brandberg is characterized by extremely high Y (up to 2,200 ppm) and low Sr (<30 ppm), resulting in the lowest Sr/Y of the six groups of silica-rich rocks (Fig. 6cd).

Extensive differentiation has depleted the Brandberg magma of Sr by fractionation of feldspar. Y, like Zr, is enriched because of delayed crystallization of zircon and other HFSE-bearing accessory minerals in these peralkaline magmas.

Nb. Nb is preferentially accommodated in rutile and to a lesser extent in magnetite, ilmenite and hornblende (Pearce and Norry, 1979; Xiong et al., 2011). Nb abundances of silica-rich granitoids are shown on Figure 7, where they are plotted in Nb-Y and Rb-Y+Nb space (Pearce et al., 1984). Nb, like Y and Zr, is high in hot, reduced magmas like those at Brandberg, Pantelleria, Nebo, and Yellowstone. In the most extreme case of the peralkaline ferroan Brandberg suite, elevated concentrations of alkalis and Cl and F contents increase the solubility of REE and high field strength elements (HFSE) (e.g., Sorensen, 1997; Keppler, 1993), allowing these elements to reach high concentration in the magma until they are removed by late-stage crystallization of zircon, ilmenite, and other HFSE-bearing minerals. Suites differentiated from more oxidized magmas, such as leucogranites of Half Dome and South Sister, crystallize magnetite and hornblende that remove Nb from the evolving magma. The Fijian trondhjemites also have low Nb contents, which, given that subduction-related magmas are characterized by low Nb, may reflect their oceanic arc to back-arc affinity (Gill et al., 1984). Granitic rocks formed by crustal melting, including Amazonia, Coyote Summit, Makalu, and Macusani, have intermediate Nb contents similar to the upper continental crustal average of 10-14 ppm (Rudnick and Gao, 2003).

Rare Earth Elements. REEs abundances from silica-rich granitoids and rhyolites range over more than two orders of magnitudes and show a wide range of patterns (Fig. 8). Silica-rich granites from Amazonia, Nebo, and Pantelleria have LREE-enriched patterns with moderate Eu anomalies. Oceanic trondhjemites, as exemplified by Udu and Wainivalau, exhibit flat patterns with REE concentrations around ten times chondrite and without Eu anomalies. The continental arc suites (Half Dome leucogranite and South Sister) exhibit moderate heavy REE depletion; Eu anomalies are weak to absent. The REE patterns for the peraluminous suites are LREE-enriched, but their precise pattern depends on the minerals participating in partial melting of metapelitic sources. The participation of REE-enriched accessory phases, such as monazite, are particularly important in controlling REE abundance and the shape of the pattern (e.g. Nabelek and Glascock, 1995). Yellowstone and Brandberg REE patterns are the most distinctive of those shown on Fig. 8. REE-enriched and relatively flat, these patterns exhibit deep, negative Eu anomalies, and have been described as “seagull” shaped by Glazner et al. (2008). Bachmann and Bergantz (2008a) postulate that the “seagull” pattern is produced by extensive fractionation of plagioclase in a hot, dry magma. REE are incompatible in pyroxene, the main ferromagnesian phase that crystallizes in these rocks. As a result, fractionation causes Eu depletion by incorporation in plagioclase whereas all other REEs increase in abundance until the point where zircon or other phases that preferentially accommodate REEs crystallize, which occurs late in the crystallization history of hot magmas.

For the six types of leucogranites, the plutonic and volcanic rocks have similar REE abundances and patterns, although Yellowstone and Brandberg patterns have deeper Eu anomalies than those of Nebo and Pantelleria (Fig. 8).

Discussion

Trondhjemites: a further subdivision

Trondhjemites, dominated by plagioclase and quartz, are uniformly calcic (Fig. 9b). However, they span a substantial range in geochemical composition, and include both ferroan and magnesian, and peraluminous and metaluminous varieties (Fig. 9a, c). Barker (1979) defined high-Al and low-Al types, and noted that Archean trondhjemites fall into the high-Al category (Fig. 9c). Trondhjemites are low-K by definition. However some of the Troodos and Wainivalau samples have extremely low-K (e.g. <0.1% K_2O)(Fig. 9e). We have chosen the Scottish Scourie gneisses to represent Archean trondhjemites. In addition to being high-Al, Scourie gneisses are magnesian, metaluminous, and exhibit HREE depleted, J-shaped, REE patterns that are common in Archean high-grade gneisses (Rollison and Windley, 1980; Rollinson and Fowler, 1987; Fig. 9). Trondhjemites from the Cornucopia stock of eastern Oregon represent a second suite of continental trondhjemites (Johnson et al., 1997). The Cretaceous Cornucopia stock is high-Al, magnesian, peraluminous, and its LREE-enriched REE patterns show no Eu anomaly (Fig. 9). Finally, two oceanic trondhjemite suites are plotted on Fig. 9: the Fijian Wainivalau plutonic suite (Stork, 1984), and trondhjemites from Troodos (Freund et al., 2014). Troodos is ferroan whereas Wainivalau is magnesian, but both of these

oceanic suites are metaluminous, low-Al, and have flat to LREE-depleted REE patterns. The four suites vary widely in Rb, Sr, and Y content (Fig. 10). Although these suites occur in diverse continental and oceanic tectonic settings and range in age from Archean to Neogene, workers agree that they originate from basaltic parents, either by partial melting (Gill et al., 1984; Johnson et al., 1997; Rollinson and Fowler, 1987), or by fractional crystallization (Freund et al., 2014).

Experimental studies provide insights into the processes that may produce the compositional variation in trondhjemites, particularly the role of water content and total pressure. Although the experimental work provides a useful guide to the conditions of trondhjemite formation, it is important to realize that the experimental systems are simplified, and that other important factors, especially fractionation and hybridization, should be considered on a case-by-case basis. Nevertheless, the experimental studies help identify the petrogenetic processes that may be responsible for three types of trondhjemites that can be distinguished based on major and trace element geochemistry. Results of low-P (<7 kb) experiments are shown on Figure 11a (Beard and Lofgren, 1991, Patiño Douce and Beard, 1995, Spulber and Rutherford, 1983; Luhr, 1990). Beard and Lofgren (1991) conducted partial melting experiments on greenstones and amphibolites from the Smartville complex at 800-1000°C and pressures up to 6.9 kb. Dehydration melting experiments contained only the water bound in hydrous phases, mainly amphiboles. In these experiments, amphibole and quartz broke down to produce pyroxenes in the restite and mildly peraluminous to metaluminous granodioritic and trondhjemitic melts. The experimental melts have compositions that plot along Barker's (1979) high-Al/low-Al boundary (Fig. 11a,c; also see Patiño Douce and Beard (1995) and

Spulber and Rutherford (1983)), and are high in iron (Fig. 11e). The partial melts obtained in water-excess experiments between 3 and 6.9 kb were quite different (Beard and Lofgren, 1991; Luhr, 1990; Figure 11a). In these experiments, plagioclase broke down, yielding an amphibole-rich restite and a strongly peraluminous melt. Alumina contents of the melts all lie within Barker's high-Al field (Fig. 11a,c) and are Fe-poor (Fig. 11e).

Rapp and Watson (1995) conducted dehydration partial melting experiments on a set of natural amphibolites at higher pressures to evaluate whether Archean trondhjemites could originate by partial melting of basaltic rocks at depth. Their results from experiments in the garnet-stable field (i.e. P>12 kb) are plotted on Figure 11b. Their starting materials included alkali basalt and olivine tholeiite. Those partial melts extracted from a garnet-bearing residue exhibit the low HREE patterns characteristic of Archean trondhjemites. The partial melts are high-Al (Fig. 11b,d), most plotting above Barker's (1979) high-Al line. FeO contents of these melts are intermediate between those produced by Beard and Lofgren's dehydration melting and water-excess melting experiments conducted at lower pressures (Fig. 11f). Note that the Scourie tonalites plot almost exclusively in the fields defined by Rapp and Watson's (1995) experimental data. These experiments suggest that some high-Al Archean trondhjemites may form by dehydration melting in the garnet stability field.

. **Archean trondhjemites** are the silica-rich end member of the Archean TTG suite. They are distinguished by high Al_2O_3 and low FeO (Fig. 11 d,f). Trace element compositions are distinctive, with extremely high Sr/Y (Fig. 10b), and J-shaped REE patterns (Fig. 9f) and plot within the fields defined by the high-pressure melting

528 experiments of Rapp and Watson (1995; Fig. 11). We note that only the granulite-facies
529 Scourie trondhjemites have low Rb (<5 ppm); amphibolite-facies Scourie trondhjemites
530 have much higher Rb (Fig. 10a). Low Rb is therefore not a primary compositional
531 characteristic of Archean trondhjemites. The Scourie trondhjemites exhibit REE patterns
532 with positive Eu anomalies, suggesting that Sr contents have been enhanced by
533 plagioclase accumulation. Their major element compositions and depletion in HREE and
534 Y suggests an origin by partial melting at high pressure, where garnet is retained in the
535 residue (Rapp et al., 1991; Rapp and Watson, 1995; Moyen and Martin, 2012). This
536 implies a thick Archean crust, although not necessarily modern-style horizontal tectonics.

537 **Peraluminous trondhjemites**, exemplified by Cornucopia, exhibit extremely
538 high Al_2O_3 and Sr contents and low FeO (Fig. 9d, 10a, 11c,e). These are best explained
539 by water-excess melting of a metabasaltic source in which plagioclase breakdown
540 accounts for the high Al and Sr in the melt but in the absence of garnet, suggesting $P < 7$
541 kb (Johnson et al., 1997; Beard and Lofgren, 1991; Luhr, 1990; Fig. 11). This process
542 could result in collisional orogens by thrusting and release of H_2O from the cold, hydrous
543 underthrust sheet and fluxes the overlying rock, as suggested by Beard (1997).

544 **Oceanic plagiogranites** are defined by the IUGS classification system as those
545 "series of plutonic rocks consisting of plagioclase, ranging in composition from
546 oligoclase to anorthite, quartz and minor amounts of hornblende and pyroxene" (Le
547 Maitre, 1989). Our representative series from Fiji and Troodos both are metaluminous, lie
548 in Barker's (1979) low-Al field, and exhibit low Sr/Y and high Y (Fig 9c,d, 10b, 11c).
549 Their low Al_2O_3 contents are consistent with low-pressure dehydration melting of
550 basaltic rocks or extreme differentiation of ocean floor basalt (Gill et al., 1984; Beard and

Lofgren, 1991; Freund et al., 2014). However, the geochemical compositions of the suites differ in a number of respects: FeO is higher and Al_2O_3, K, and Rb are lower in Troodos samples (Fig. 10a; 11c,e). The K and Rb depletions could result from evolution of a late fluid phase (Beard, 1998). The geochemical variations exhibited by a host of plagiogranite suites—Troodos and Fiji among them—have spurred a vigorous debate on the origins of plagiogranite. Models include partial melting of gabbroic crust, fractional crystallization of parental basalt, and also include the possible role of liquid immiscibility, and assimilation and partial melting of hydrothermally altered oceanic crust (Koepke et al., 2007). It is likely, as observed by Rollinson (2009), that a number of different processes are involved in the production of silicic magmas within mafic oceanic crust, but their common origin from mafic sources produce in all cases calcic, low-Al, silica-rich rocks.

Implications

In this paper, we have shown that using major and trace element geochemistry it is possible to identify six geochemically distinct groups of silica-rich granitoids and their eruptive equivalents. Each of these groups can be subdivided in turn, as we've shown above for trondhjemites, and in an earlier paper, for ferroan granites (Frost and Frost, 2011). The major element geochemistry of a silica-rich granitoid provides important information on the main minerals in the rock: Fe-index relates to the compositions of the ferromagnesian silicates and the modified alkali-lime index relates to the compositions of the feldspars. The aluminum saturation index and alkali index relate to the relative

574 abundances of aluminum and alkalis. Changes in trace element abundances give
575 important information about the source of the original magma, the differentiation history
576 of the melt, and the identity of minor phases that were likely present in cumulates and
577 restite. All these data provide basic yet critical information for petrologists working on
578 problems relating to granite petrology.

579 Geochemical classification schemes have also been used to identify tectonic
580 environment (i.e. Pearce et al., 1984). We recommend caution in this regard because the
581 composition of granitic rocks is controlled by the composition of rocks that are melting or
582 differentiating rather than by the tectonic environment. For example, melting of granitic
583 gneiss in an arc environment is likely to produce the same composition of melt as melting
584 of the same composition crust in a rifting environment. ,A specific example is provided
585 by the Johnson Granite Porphyry, the youngest unit of the Tuolumne intrusion formed in
586 a continental arc, and the Bishop tuff, a product of rifting. Despite the different
587 environments, both of these silica-rich units are mainly magnesian and calc-alkalic (Fig.
588 12), and their Rb and Zr contents are comparable (Hildreth and Wilson, 2007).
589

590 **Are silica-rich granites equivalent to silica-rich rhyolites?**

591 The cumulate nature of granitic rocks has been documented by many studies
592 showing that adjacent or zoned crystals must have grown in different times and places
593 and equilibrated with different mineral and magma compositions (e.g., Marsh and
594 Maxey, 1985; Zen, 1986; Mahood, 1990; Gagnevin et al., 2005). Recent models envision
595 the formation of granitic plutons from silicic crystal mushes (e.g. Bachmann and
596 Bergantz, 2004). At early stages of solidification, crystals may be kept in suspension by

convection. As crystallization continues, crystals form a framework, impeding convection. Interstitial rhyolitic liquid, if extracted and erupted, will be petrologically linked to the plutonic rocks, but it may be more silica-rich and show a stronger crystal fractionation signature than the intrusive cumulate rocks from which they were extracted (Bachmann and Bergantz, 2004, 2006, 2008ab, Burgisser and Bergantz, 2011). An example of such a process includes the plutonic and volcanic rocks of the Latir volcanic field, in which intermediate volcanic and plutonic rocks are nearly identical in major, trace, and Sr, Nd, and Pb isotopic compositions, but in which the highly evolved rocks have different REE suggesting a contrast in the role of accessory minerals in the evolution of the plutonic and volcanic suites. (Johnson et al., 1989).

Another important difference between plutonic rocks and rhyolites relates to the timescale of formation. Plutonic complexes are the result of what may be a series of multiple intrusive events and varied differentiation processes acting over relatively long periods of time, whereas a rhyolite flow or tuff records a single eruptive event. This is illustrated by comparing the peraluminous plutonic suite of Harney Peak, in which multiple intrusions formed by partial melting of heterogeneous crustal sources produce a range in MALI, Fe-index, and ASI (Nabelek et al., 1992; Nabelek and Bartlett, 1998), with the peraluminous ash-flow tuffs at Macusani, in which the major element chemistry and the mineral chemistry of the eruptive units is essentially constant, indicating minimal fractional crystallization occurred (Pichavant et al., 1988ab).

One difficulty in comparing silica-rich rhyolites and granites is the scarcity of occurrences where both intrusive and extrusive suites from a single magmatic system are exposed. Without such direct comparators it can be difficult to assess whether silica-rich

620 rhyolites are in fact compositionally distinct from their plutonic complements. One
621 volcanic system that erupted samples of plutonic material is ignimbrite from the Cerro
622 Galán caldera on the eastern edge of the Puna plateau (Folkes et al., 2011). The
623 ignimbrite contains rhyodacite pumice clasts, interpreted as erupted crystal mushes,
624 which are composed mainly of matrix glass, plagioclase, biotite, and quartz. SiO_2 of most
625 samples lie between 68.5 and 70.5%. Matrix glass has higher silica, up to 81%, indicating
626 that interstitial liquid was highly evolved (Folkes et al., 2011). If silica-rich rhyolites
627 form by separation of evolved liquid from crystal cumulates during eruption, then
628 rhyolites and granites will not have identical compositions. In reality, the plutonic
629 complements to erupted liquids are composed of mixtures of crystals and interstitial melt
630 (Lee and Morton, 2015), lessening the compositional difference between extrusive and
631 intrusive components of a magmatic system.

632 Because of the scarcity of complexes that expose both volcanic and plutonic
633 samples, other studies have compared volcanic and plutonic rocks of various ages,
634 locations, and tectonic setting. For example, Halliday et al. (1991), suggested that
635 rhyolites with Rb/Sr ratios > 100 have no plutonic equivalent. They reached this
636 conclusion by comparing ferroan alkali-calcic rhyolites, including Yellowstone, Glass
637 Mountain, and the mildly peralkaline Sierra La Primavera, with magnesian Cordilleran
638 and Caledonian intrusions, such as the Peru Coastal batholith and Donegal granites. Had
639 they compared these rhyolites with ferroan alkali-calcic to peralkaline plutonic rocks
640 (such as Nebo and Brandberg, Fig. 4a), their conclusion would have been different.

641 Similarly, Glazner et al. (2008) concluded that there was no genetic relationship
642 between high-silica rhyolites and granodiorite plutons because aplites from the Sierra

643 Nevada batholith were compositionally distinct from high-silica rhyolites. The high-
644 silica rhyolites they used for comparison were all ferroan alkali-calcic suites, whereas the
645 Sierra Nevada batholith is a magnesian calc-alkalic to calcic pluton. Unsurprisingly, the
646 Sierran aplites share high Sr/Y characterisitic of continental arc batholiths, whereas the
647 high-silica rhyolites have much lower Sr/Y, similar to the ferroan alkali-calcic suites
648 shown on Fig. 6. The distinctive U-shaped REE pattern of the Sierran aplites indicates
649 that titanite crystallized, depleting these liquids of middle REEs. Titanite is a common
650 accessory phase in subduction-related batholiths but is not typical of hot, dry, ferroan
651 magmas (Bachmann and Bergantz, 2008a) that evolve very different, gull-wing REE
652 patterns.

653 A different conclusion was suggested by Hildreth (2004), who also discussed the
654 relationship between leucogranites and rhyolites. Hildreth (2004) proposed that the
655 Bishop Tuff is underlain by a Quaternary granitoid pluton equivalent in size to older
656 Sierran plutons. He furthermore noted the compositional similarity of Bishop Tuff and
657 Sierran leucogranites, and interpreted the latter as analogous to the plutonic “crystallized
658 remainders” left in the subsurface following eruption of the ignimbrites. This comparison
659 suggests that unerupted equivalents to silica-rich rhyolites do exist in the plutonic rock
660 record. Even though Hildreth (2004) compares igneous rocks from different tectonic
661 environments (continental arc versus rift) the comparison is valid because, as noted
662 above, the parental magmas were compositionally similar. These examples illustrate the
663 importance of making comparisons and interpretations among and between extrusive and
664 intrusive suites using the classification of silica-rich rhyolites and granites outlined in this
665 paper. We have shown that although silica-rich rocks are dominated by quartz and

feldspars, their major and trace element compositions nevertheless vary sufficiently to distinguish suites of different parentage and petrogenesis. Modern petrology makes use of various microanalytical elemental and isotopic techniques to elucidate petrogenetic processes of differentiation, assimilation, magma mixing and mingling, and the timescales and kinetics of these processes. These investigations are best generalized based on a firm understanding of the lineage of the magmatic system, which is preserved in the whole rock major and trace element geochemistry of the rocks.

Acknowledgements

C.D. Frost and B.R. Frost gratefully acknowledge support for this study provided by NSF grant EAR 0537670. This manuscript was completed while CDF was serving at the National Science Foundation.

References Cited

Adam, J., Green, T.H., Soey, H.S., and Ryan, C.G. (1997) Trace element partitioning between aqueous fluids, silicate melts, and minerals. European Journal of Mineralogy, 9, 569-584.

Arth, J. G. (1976) Behavior of trace elements during magmatic processes – a summary of theoretical models and their applications. Journal of Research of the U.S. Geological Survey, 4, 41-47.

Avanzinelli, R., Bindi, L., Menchetti, S., and Conticelli, S. (2004) Crystallisation and genesis of peralkaline magmas from Pantelleria Volcano, Italy: an integrated petrological and crystal-chemical study. Lithos, 73, 41-69.

689 Bachmann, O., and Bergantz, G.W. (2004) On the origin of crystal-poor rhyolites:
690 Extracted from batholithic crystal mushes. Journal of Petrology, 45, 1565-1582.
691 Bachmann, O., and Bergantz, G.W. (2006) Gas percolation in upper-crustal silicic crystal
692 mushes as a mechanism for upward heat advection and rejuvenation of near-solidus
693 magma bodies. Journal of Volcanology and Geothermal Research, 149, 85-102.
694 Bachmann, O., and Bergantz, G.W. (2008a) Rhyolites and their source mushes across
695 tectonic settings. Journal of Petrology, 49, 2277-2285.
696 Bachmann, O., and Bergantz, G.W. (2008b) The magma reservoirs that feed
697 supereruptions. Elements, 4, 17-21.
698 Barker, F. (1979) Trondhjemite; definition, environment, and hypotheses of origin. In
699 Barker, F., ed. Trondhjemites, dacites, and related rocks. Elsevier, Amsterdam, 1-12.
700 Basaltic Volcanism Study Project (1981) Basaltic volcanism on the terrestrial planets.
701 New York, Pergamon Press, 1286 pp.
702 Bateman, P. C., and Chappell, B. W. (1979) Crystallization, fractionation and
703 solidification of the Tuolumne Intrusive series, Yosemite National Park, California.
704 Geological Society of American Bulletin, 90. 465-482.
705 Bea, F. (1996) Residence of REE, Y, Th, and U in granites and crustal protoliths,
706 implications for the chemistry of crustal melts. Journal of Petrology, 37, 521-552.
707 Beard, J. S. (1998) Polygenetic tonalite-trondjhemite-granodiorite (TTG) magmatism in
708 the Smartville Complex, Northern California with a note on LILE depletions in
709 plagiogranites. Mineralogy and Petrology, 64, 15-45.
710 Beard, J.S. (1997) Geochemistry and petrogenesis of tonalite dikes in the Smith River
711 allochthon, south-central Virginia, *in* Sinha, A.K., Whalen, J.B., and Hogan, J.P.,

712 eds., The Nature of Magmatism in the Appalachian Orogen. Geological Society of
713 America Memoir 191, 75-86.
714 Beard, J.S., and Lofgren, G.E. (1991) Dehydration melting and water-saturated melting
715 of basaltic and andesitic greenstones and amphibolites at 1, 3, and 6.9 kb. Journal of
716 Petrology, 32, 365-401.
717 Best, M.G., Gromme, S., Deino, A.L., Christiansen, E.H., Hart, G.L., and Tingey, D.G.
718 (2013) The 36-18 Ma Central Nevada ignimbrite field and calderas, Great Basin,
719 USA: Multicyclic super-eruptions. Geosphere, 9, 1562-1636.
720 Blundy, J.E., and Wood, B.J. (1991) Crystal-chemical controls on the partitioning of Sr
721 and Ba between plagioclase feldspar, silicate melts and hydrothermal solutions.
722 Geochimica et Cosmochimica Acta, 55, 191 – 209.
723 Brophy, J.G., and Dreher, S.T. (2000) The origin of composition gaps at South Sister
724 volcano, central Oregon: implications for fractional crystallization processes beneath
725 active calc-alkaline volcanoes. Journal of Volcanology and Geothermal Research,
726 102, 287-307.
727 Burgisser, A., and Bergantz, G.W. (2011) A rapid mechanism to remobilize highly
728 crystalline magma bodies. Nature, 471, 212-215.
729 Coleman, D. S., Bartley, J.M., Glazner, A.F., and Pardue, M.J., (2012) Is chemical
730 zonation in plutonic rocks driven by changes in source magma composition or
731 shallow-crustal differentiation? Geosphere; 8, 1568–1587.
732 Dall'Agnol, R., and Oliveira, D.C. (2007) Oxidized, magnetite-series, rapakivi-type
733 granites of Carajás, Brazil: Implications for classification and petrogenesis of A-type
734 granites. Lithos, 93, 215-233.

735 Defant, M.J., and Drummond, M.S. (1990) Derivation of some modern arc magmas by
736 melting of young subducted lithosphere. Nature, 347, 662-665.
737 Fierstein, J., Hildreth, W., and Calvert, A.T. (2011) Eruptive history of South Sister,
738 Oregon Cascades, Journal of Volcanology and Geothermal Research, 207, 145-179.
739 Folkes, C.B., de Silva, S.L., Wright, H.M., and Cas, R.A.F. (2011) Geochemical
740 homogeneity of a long-lived, large silicic system; evidence from the Cerro Galán
741 caldera, NW Argentina. Bulletin of Volcanology, 73, 1455-1486.
742 Freund, S., Haase, K.M., Keith, M., Beier, C., Garbe-Schönberg, D. (2014) Constraints
743 on the formation of geochemically variable plagiogranite intrusions in the Troodos
744 Ophiolite. Contributions to Mineralogy and Petrology, 167, 978-1000.
745 Frost, B.R., Arculus, R.J., Barnes, C.G., Collins, W.J., Ellis, D.J., and Frost, C.D. (2001)
746 A geochemical classification of granitic rocks. Journal of Petrology, 42, 2033-2048.
747 Frost, B.R., and Frost, C.D. (2008) A geochemical classification for feldspathic igneous
748 rocks. Journal of Petrology, 49, 1955-1969.
749 Frost, C.D., and Frost, B.R. (2011) On Ferroan (A-type) Granitoids: their compositional
750 variability and modes of origin. Journal of Petrology, 52, 39-53.
751 Gagnevin, D., Daly, J.S., Poli, G., and Morgan, D. (2005) Microchemical and Sr isotopic
752 investigation of zoned K-feldspar megacrysts: insights into the petrogenesis of a
753 granitic system and disequilibrium crystal growth. Journal of Petrology, 46, 1689-
754 1724.
755 Gill, J.B., Stork, A.K., and Whelan, P.W. (1984) Volcanism accompanying back-arc
756 basin development in the southwest Pacific. Tectonophysics, 102, 207-224.

757 Glazner A.F., Coleman, D.S., and Bartley, J.M. (2008) The tenuous connection between
758 high-silica rhyolites and granodiorite plutons. Geology, 26, 183-186.
759 Halliday, A.N., Davidson,J.P., Hildreth, W., and Holden, P. (1991) Modelling the
760 petrogenesis of high Rb/Sr silicic magmas. Chemical Geology, 92, 107-114.
761 Hildreth, W. (2004) Volcanogenic perspectives on Long Valley, Mammoth Mountain,
762 and Mono Craters: several contiguous but discrete systems. Journal of Volcanology
763 and Geothermal Research, 136, 169-198.
764 Hildreth, W., and Wilson, C.J.N. (2007) Compositional zonation of the Bishop Tuff.
765 Journal of Petrology, 48, 951-999.
766 Hildreth, W., Halliday, A.N., and Christiansen, R.L. (1991) Isotopic and chemical
767 evidence concerning the genesis and contamination of basaltic and rhyolitic magma
768 beneath the Yellowstone plateau volcanic field. Journal of Petrology, 32, 63-138.
769 Hill, M., Barker, F., Hunter, D., and Knight, R. (1996) Geochemical characteristics and
770 origin of the Lebowa granite suite, Bushveld Complex. International Geology
771 Review, 38, 195-227.
772 Holtz, P. E. (1971) Plutonic Rocks of the Klamath Mountains, California and Oregon. US
773 Geological Survey Professional Paper 648-B, 20 pp.
774 Johnson, C.M., Czamanske, G.K., and Lipman, P.W. (1989) Geochemistry of intrusive
775 rocks associated with the Latir volcanic field, New Mexico, and contrasts between
776 evolution of plutonic and volcanic rocks. Contributions to Mineralogy and Petrology,
777 103, 90-109.

778 Johnson, K., Barnes, C.G., and Miller, C.A. (1997) Petrology, Geochemistry and genesis
779 of High-Al tonalite and trondjhemites of the Cornucopia stock, Blue Mountains,
780 Northeastern Oregon, Journal of Petrology, 38, 1585-1611.
781 Keppler, H. (1993) Influence of fluorine on the enrichment of high field strength
782 elements in granitic rocks. Contributions to Mineralogy and Petrology, 114, 479-488.
783 Kleeman, G.J., and Twist, D. (1989) The compositionally zoned sheet-like granite pluton
784 of the Bushveld Complex: Evidence bearing on the nature of A-type magmatism.
785 Journal of Petgrology, 30, 1383-1414.
786 Koepke, J., Berndt, J., Feig, S.T., Holtz, F. (2007) The formation of SiO_2-rich melts
787 within the deep oceanic crust by hydrous partial melting of gabbros. Contributions to
788 Mineralogy and Petrology, 153, 67-84.
789 Korringa, M.K. and Nobel, D.C. (1970) Distribution of Sr and Ba between natural
790 feldspar and igneous melt. Earth and Planetary Science Letters, 11, 147-151.
791 Le Bas, M.J., Le Maitre, R.W., Streckeisen, A., and Zanettin, B.A. (1986) Chemical
792 classification of volcanic rocks based on the total alkali-silica diagram. Journal of
793 Petrology, 27, 745-750.
794 Le Maitre, R.W. (1989) A classification of the igneous rocks and glossary of terms.
795 Blackwell, Oxford, p. 193.
796 Lee, C-T. A., and Morton, D.M. (2015) High silica granites: terminal porosity and crystal
797 settling in shallow magma chambers. Earth and Planetary Science Letters, 409,
798 23-31.

799 Long, P. E. (1978) Experimental determination of partition coefficients for Rb, Sr, and
800 Ba between alkali feldspar and silicate liquid. Geochimica et Cosmochima Acta, 42,
801 833-846.
802 Luhr, J.F. (1990) Experimental phase relations of water- and sulfur-saturated arc magmas
803 and the 1982 eruptions of El Chichon Volcano. Journal of Petrology, 31, 1071-1114.
804 Mahood, G.A. (1990) Second reply to comment of R.S.J. Sparks, H.E. Huppert & C.J.N.
805 Wilson on 'Evidence for long residence times of rhyolitic magma in the Long Valley
806 magmatic system: the isotopic record in precaldera lavas of Glass Mountain'. Earth
807 and Planetary Science Letters, 99, 395-399.
808 Mahood, G. and Hildreth, W. (1983) Large partition coefficients for trace elements in
809 high-silica rhyolites. Geochimica et Cosmochima Acta, 47, 11-30.
810 Marsh, B.D., and Maxey, M.R. (1985) On the distribution and separation of crystals in
811 convecting magma, Journal of Volcanology and Geothermal Research, 24, 95-150.
812 Martin, H. (1999) Adakitic magmas: modern analogues of Archaean granitoids. Lithos,
813 46, 411-429.
814 Mathez, E.A., VanTongeren, J.A., Schweitzer, J. (2013) On the relationships between the
815 Bushveld Complex and its felsic roof rocks, part 1: petrogenesis of Rooiberg and
816 related felsites. Contributions to Mineralogy and Petrology, 166, 435-449.
817 McCurry, M., Hayden, K.P., Morse, L.H., and Mertzman, S. (2008) Genisis of post-
818 hotspot, A-type rhyolite of the Eastern Snake River Plain volcanic field by extreme
819 fractional crystallization of olivine tholeiite. Bulletin of Volcanology, 10, 361-383.
820 Moyen, J.-F. (2009) High Sr/Y and La/Yb ratios; the meaning of the "adakitic signature."
821 Lithos, 112, 556-574.

822 Moyen, J.-F. and Martin, H.. (2012) Forty years of TTG research. Lithos, 148, 312-336.
823 Nabelek, P.I., and Bartlett, C.D. (1998) Petrologic and geochemical links between the
824 post-collisional Proterozoic Harney Peak leucogranite, South Dakota, USA, and its
825 source rocks. Lithos, 45, 71-85.
826 Nabelek, P.I., and Glascock, M.D. (1995) REE-depleted leucogranites, Black Hills, South
827 Dakota: a consequence of disequilibrium melting of monazite-bearing schists. Journal
828 of Petrology, 36, 1055-1071.
829 Nabelek, P. I., Russ-Nabelek, C., and Denison, J. R. (1992) The generation and
830 crystallization conditions of the Proterozoic Harney Peak Leucogranites, Black Hills,
831 South Dakota, USA: petrologic and geochemical constraints. Contributions to
832 Mineralogy and Petrology, 110, 173-191.
833 Nardi, L.V.S., Formoso, M.L.L., Müller, I.F., Fontana, E., Jarvis, K., Lamarão, C. (2013)
834 Zircon/rock partition coefficients of REEs, Y, Th, U, Nb, and Ta in granitic rocks:
835 uses for provenance and mineral exploration purposes. Chemical Geology, 335, 1-7.
836 Nash, W.P. and Crecraft, H.R. (1985) Partition coefficients for trace elements in silicic
837 magmas. Geochimica et Cosmochimica Acta, 49, 2309-2322.
838 Neave, D.A., Fabbro, G., Herd, R.A., Petrone, C.M., and Edmonds, M. (2012) Melting,
839 differentiation and degassing at the Pantelleria volcano, Italy, Journal of Petrology,
840 53, 637-663.
841 Oliveira, D.C., Dall'Agnol, R., Barros, C.E.M., and Oliveira, M.A. (2009) Geology,
842 geochemistry and magmatic evolution of the Paleoproterozoic, anorogenic oxidized
843 A-type Redenção granite of the Jamon suite, eastern Amazonian craton, Brazil. The
844 Canadian Mineralogist, 47, 1441-1468.

845 Patiño Douce, A. (1997) Generation of metaluminous A-type granites by low-pressure
846 melting of calc-alkaline granitoids. Geology, 25, 743-746.
847 Patiño Douce A. E., and Beard, J.S. (1995) Dehydration melting of biotite gneiss and
848 quartz amphibolite from 3 to 15 kbars. Journal of Petrology, 36, 707-738.
849 Patiño Douce A. E., and Harris, N. (1998) Experimental constraints on Himalayan
850 anatexis. Journal of Petrology, 39, 689-710.
851 Peacock, M.A. (1931) Classification of igneous rock series. Journal of Geology, 39, 54-
852 67.
853 Pearce, J.A., and and Norry, M.J. (1979) Petrogenetic implications of Ti, Zr, Y, and Nb
854 variations in volcanic rocks. Contributions to Mineralogy and Petrology, 69, 33-47.
855 Pearce, J.A., Harris, N.B.W., and Tindle, A.G. (1984) Trace element discrimination
856 diagrams for the tectonic interpretation of granitic rocks. Journal of Petrology, 25,
857 956-983.
858 Pichavant, M., Kontak, D.J., Briqueu, L., Valencia Herrera, J., and Clark, A. H. (1988b)
859 The Miocene-Pliocene Macsani Volcanics, SE Peru II. Geochemistry and origin of a
860 felsic peraluminous magma. Contributions to Mineralogy and Petrology, 100, 325-
861 338.
862 Pichavant, M., Kontak, D.J., Herrera, J.V., and Clark, A.H. (1988a) The Miocene-
863 Pliocene Macusani Volcanics, SE Peru I. Mineralogy and magmatic evolution of a
864 two-mica aluinosilicate-bearing ignimbrite suite. Contributions to Mineralogy and
865 Petrology, 100, 300-324.

866 Rapp, R.P., and Watson EB (1995) Dehydration melting of metabasalt at 8–32 kbar:
867 implications for continental growth and crust-mantle recycling. Journal of Petrology,
868 36, 891–931.
869 Rapp, R.P., Watson, E.B., and Miller, C.F. (1991) Partial melting of amphibolite/eclogite
870 and the origin of Archean trondhjemites and tonalites. Precambrian Research, 51, 1-
871 25.
872 Rollinson, H. (2009) New models for the genesis of plagiogranites in the Oman ophiolite.
873 Lithose, 112, 603-634.
874 Rollinson, H.R. and Fowler, M.B. (1987) The magmatic evolution of the Scourian
875 complex at Gruinard Bay in Park, R.G. and Tarney, J. (eds) Evolution of the
876 Lewisian and Comparable Precambrian High Grade Terranes. Geological Society of
877 London Special Publication 27, 57-71.
878 Rollinson, H.R. and Windley, B.F. (1980) An Archean granulite-grate tonalite-
879 trondhjemite-granite suite from Scourie, NW Scotland: Geochemistry and origin.
880 Contributions to Mineralogy and Petrology, 72, 265-281.
881 Rudnick, R.L, and Gao, S. (2003) Composition of the Continental Crust, In The Crust,
882 ed. R.L. Rudnick, Treatise on Geochemistry vol. 3, eds. H.D. Holland and K.K.
883 Turekian, Oxford, Elsevier-Pergamon, pp 1-64.
884 Sawka, W.N., Chappell, B.W., Kistler, R.W. (1990) Granitoid compositional zoning by
885 side-wall boundary layer differentiation; evidence from the Palisade Crest intrusive
886 suite, central Sierra Nevada, California. Journal of Petrology, 31, 519-553.
887 Schmitt, A.K., Emmermann, R., Trumbull, R.B., Bühn, B., and Henjes-Kunst, F. (2000)
888 Petrogenesis and $^{40}Ar/^{39}Ar$ geochronology of the Brandberg Complex, Namibia:

Evidence for a major mantle contribution in metaluminous and peralkaline granites. Journal of Petrology, 41, 1207-1239.

Shand, S.J. (1927) The eruptive rocks. New York: D. Van Nostrand Co., 360 pp.

Skjerlie, K.P., and Johnston, A.D. (1993) Fluid-absent melting behavior of an F-rich tonalitic gneiss at mid-crustal pressures: Implications for the generation of anorogenic granites. Journal of Petrology, 34, 785-815.

Sorensen, H. (1997) The agpaitic rocks; an overview. Mineralogical Magazine, 61, 485-498.

Spulber, S.D., and Rutherford, M.J. (1983) The origin of rhyolite and plagiogranite in the oceanic crust: an experimental study. Journal of Petrology, 24, 1-25.

Stelten, M.E., and Cooper, K.M. (2012) Constraints on the nature of the subvolcanic reservoir at South Sister volcano, Oregon from U-series dating combined with sub-crystal trace-element analysis of plagioclase and zircon. Earth and Planetary Science Letters, 313-314, 1-11.

Stork, A.L. (1984) Silicic magmatism in an Island Arc, Fiji, Southwest Pacific: Implications for Continental Growth. Ph.D. dissertation, University of California, Santa Cruz, 273 pp.

Taylor, S.R., and McLennan, S.M. (1985) The continental crust: its composition and evolution. Oxford, Blackwell Scientific Publications, 312 pp.

Visona, D., and Lombardo, B. (2002) Two-mica and tourmaline leucogranites from the Everest-Makalu region (Nepal-Tibet). Himalayan leucogranite genesis by isobaric heating? Lithos, 62, 125-150.

911 Watson, E.B. (1979) Zircon saturation in felsic liquids: experimental results and
912 applications to trace element geochemistry. Contributions to Mineralogy and
913 Petrology, 70, 407-419.
914 Watson, E.B., and Harrison, T. M. (1983) Zircon saturation revisited: temperature and
915 composition effects in a variety of crustal magma types. Earth and Planetary Science
916 Letters, 64, 295-304.
917 Weiss, S., and Troll, G. (1989) The Ballachulish igneous complex, Scotland:
918 petrography, mineral chemistry, and order of crystallization in the monzodiorite-
919 quartz diorite suite and in the granite. Journal of Petrology 30, 1069-1115.
920 Whalen, J.B., and Currie, K.L. (1984) The Topsails igneous terrane, Western
921 Newfoundland: Evidence for magma mixing, Contributions to Mineralogy and
922 Petrology, 87, 319-327.
923 Whalen, J.B., Jenner, G.A., Longstaff, F.J., Robert, F., and Gariépy, C. (1996)
924 Geochemical and isotopic (O,Nd, Pb, and Sr) eonstrains on A-type granite
925 petrogenesis based on the Topsails Igneous Suite, Newfoundland Appalachians.
926 Journal of Petrology, 37, 1463-1489.
927 White, J.C., Parker, D.F., and Ren, M. (2009) The origin of trachyte and pantellerite from
928 Pantelleria, Italy: Insights from major element, trace element, and thermodynamic
929 modeling. Journal of Volcanology and Geothermal Research, 179, 33-55.
930 Xiong, X., Keppler, H., Audétat, A., Ni, H., Sun, W., Li, Y. (2011) Partitioning of Nb
931 and Ta between rutile and felsic melt and the fractionation of Nb/Ta during partial
932 melting of hydrous metabasalt. Geochemica et Cosmochimica Acta, 75, 1673-1692.

933 Yang, P. and Rivers, T. (2000) Trace element partitioning between existing biotite and
934 muscovite from metamorphic rocks, Western Labrador: Structural, compositional and
935 thermal controls. Geochimica et Cosmochimica Acta, 64, 1451-1472.
936 Zen, E.A. (1986) Aluminum enrichment in silicate melts by fractional crystallization:
937 Some mineralogic and petrographic constraints. Journal of Petrology, 27, 1095-1117.
938
939
940
941 **Figure captions**
942 **Fig. 1.** Relationship of major element geochemistry to mafic mineral abundance for
943 representative plutons. a. Variation of color index (mafic mineral mode) with respect to
944 the sum of ferromagnesian oxides (TiO_2 + Fe_2O_3 + FeO + MnO + MgO). b. Variation of
945 color index with silica. Only half of the rocks with $SiO_2 \geq 70\%$ have $\leq 5\%$ mafic
946 minerals, by volume. Data from Bateman and Chappell (1979); Holtz (1971); Johnson et
947 al. (1997); Sawka et al. (1990); Weiss and Troll (1989); and Whalen et al. (1996).
948
949 **Fig. 2.** Variation diagrams showing the geochemical characteristics of silica-rich rock
950 suites inferred to have formed primarily by crustal melting. 2a,b,c = plutonic rocks,
951 2d,e,f = volcanic rocks. Sources of data are given on Table 2.
952
953 **Fig. 3**. Diagrams showing the geochemical characteristics of silica-rich rock suites
954 inferred to have formed primarily by differentiation. 3a,b,c = plutonic rocks, 3d,e,f =
955 volcanic rocks. Both granodiorites (pale orange) and leucogranites (orange) are plotted

from Half Dome because the granodiorite compositions are used as the starting composition for crystallization models shown in Figure 4c. In figure 3f, field of samples from Pantelleria extends to ASI as low as 0.5. Sources of data are given on Table 2.

Fig. 4. Variations of Rb and Sr in silica-rich rock suites. a. Suites inferred to have formed dominantly by fractional crystallization. b. Suites inferred to have formed by crustal melting. c. Comparison of the fields outlined by Rb and Sr compositions of rocks from Fig. 4a with trends followed by Rayleigh crystallization (solid heavy lines) and equilibrium batch melting (heavy dashed lines) of a model alkali basalt and the Half Dome granodiorite as calculated by the methods of Halliday et al. (1991). d. Comparison of the fields outlined by Rb and Sr compositions of rocks from Fig. 4b with trends followed by fractional crystallization (solid heavy lines) and batch melting (heavy dashed lines) of shale and average upper crust as calculated by the methods of Halliday et al. (1991). Sources of data shown in Fig. 4a and 4b are listed on Table 2. Upper crust from Taylor and McLennan (1985), Hualalai, Hawaii alkali basalt from Basaltic Volcanism Study (1981), pelite from Nabelek and Bartlett (1988), and Half Dome leucogranite from Coleman et al. (2012).

Fig. 5. Variations of Zr concentration in melts of various compositions as calculated from the expression of Watson and Harrison (1983). Note that the Zr content of glasses from the peralkaline lavas of Pantelleria, which are inferred to have formed at 800°C to 870°C (Neave et al., 2012), lie far above these curves, exemplifying the strong enrichment of Zr in peralkaline rocks.

979

980 **Fig. 6.** Diagrams depicting selected trace element compositions of silica-rich plutonic
981 (Figs 6a, b) and volcanic rocks (Figs. 6c,d). Sources of data are listed on Table 2.

982

983 **Fig. 7**. Trace element discrimination diagrams after Pearce et al. (1984) for silica-rich
984 plutonic (Fig. 7a,b) and volcanic (Fig. 7c,d) suites. COLG = collisional granites, ORG =
985 ocean ridge granites, VAG = volcanic arc granites, WPG = within plate granites. Sources
986 of data are listed on Table 2.

987

988 **Fig. 8.** Chondrite-normalized rare earth element diagrams for silica-rich plutonic (Figs.
989 7a,b,c) and volcanic (Figs. 7d,e,f) rocks. Sources of data are listed on Table 2.

990

991 **Fig. 9.** Diagrams showing the compositional trends in four occurrences of silica-rich
992 trondhjemitic rocks. Data from Stork (1984), Freund et al., (2014), Johnson et al., 1997;
993 Rollinson and Fowler (1987), and Rollinson and Windley (1980).

994

995 **Fig. 10.** Diagrams depicting the variations of minor elements in silica-rich trondjhemites.
996 Sources of data are as in Fig. 9.

997

998 **Fig. 11.** Compositions of melts produced by experimental melting of mafic rocks. Fig.
999 9a, Results of dehydration melting and water-excess melting at moderate to low pressures
1000 (Beard and Lofgren, 1991, Patino Douce and Beard, 1995, Spulber and Rutherford, 1983;
1001 Luhr, 1990). Fig. 9b. Results of garnet present dehydration melting experiments at higher

pressure Rapp and Watson (1995). Fig. 9c,e. Comparison of Cornucopia, Fiji, and Troodos trondhjemites with fields for experimental results from low to moderate pressures. Fig. 9d,f. Comparison of Scourie trondhjemites with fields for experimental results at high pressures.

Fig. 12. Diagrams comparing the major element composition of the Johnson granite porphyry (circles) to "normal" pumice from the Bishop tuff (field; data from Hildreth and Wilson, 2007). The vast majority of the 255 Bishop pumice compositions lie adjacent to Johnson granite porphyry samples.

1012

Table 1: Geochemical indices for classification of granitic rocks	
Index	**Definition**
Fe-index[1,2]	Boundary between ferroan and magnesian: $FeO^*/(FeO^* + MgO) = 0.46 + 0.005*SiO_2$
Modified alkali-lime index (MALI)[2]	Boundary between alkalic and alkali-calcic: $Na_2O + K_2O - CaO = -41.86 + 1.112*SiO_2 - 0.00572*SiO_2^2$ Boundary between alkali calcic and calc-alkalic: $Na_2O + K_2O - CaO = -44.72 + 1.094*SiO_2 - 0.00527*SiO_2^2$ Boundary between calc-alkalic and calcic: $Na_2O + K_2O - CaO = -45.36 + 1.0043*SiO_2 - 0.00427*SiO_2^2$
Aluminum-saturation index (ASI)[3,4]	ASI = Al/(Ca – 1.67P + Na + K) on a molecular basis; peraluminous rocks have ASI > 1; metaluminous and peralkaline rocks have ASI < 1
Alkalinity index (AI)[3]	AI = Al – (K + Na) on a molecular basis; peralkaline rocks have AI < 0; metaluminous and peraluminous rocks have AI > 0

1013

1014 References: [1]Frost et al. (2008); [2]Frost et al. (2001); [3]Shand (1927); [4]Zen (1986).

1015

1016

1017

Table 2: Six groups of silica-rich granitoids			
Group	**Process**	**Plutonic example**	**Volcanic example**
1) Peraluminous leucogranites	*Partial melting of pelitic rocks*	Makalu[1]	Macusani[2]
2) Ferroan calc-alkalic	*Partial melting of tonalite or granodiorite*	Amazonia granites[3]	Coyote Summit[4]
3) Trondhjemite (magnesian-calcic)	*Partial melting and/or differentiation of basaltic rocks*	Wainivalau pluton, Fiji[5]	Udu volcanics, Fiji[5]
4) Ferroan alkali-calcic	*Partial melting and/or differentiation of tholeiite*	Nebo Granite[6, 7]	Yellowstone[8]
5) Magnesian calc-alkalic or calcic	*Differentiation of high-Al basalt or andesite.*	Half Dome leucogranite, Tuolumne[9]	South Sister[10, 11]
6) Peralkaline ferroan	*Differentiation of transitional or alkali basalt*	Brandberg[12]	Pantelleria[13, 14]

1018

1019 Sources of data: 1. Visona and Lombardo, 2002; 2. Pichavant et al., 1988b; 3. Dall'Agnol
1020 and Oliveira, 2007; 4. Best et al., 2013; 5. Stork, 1984; 6. Kleeman and Twist, 1989; 7.
1021 Hill et al., 1996; 8, Hildreth et al., 1991; 9. Coleman et al., 2012; 10. Fierstein et al.,
1022 2011; 11. Brophy and Dreher, 2000; 12. Schmitt et al., 2000; 13. Avanzinelli et al, 2004;
1023 14. White et al., 2009.

1024

1025 .

1026

1027

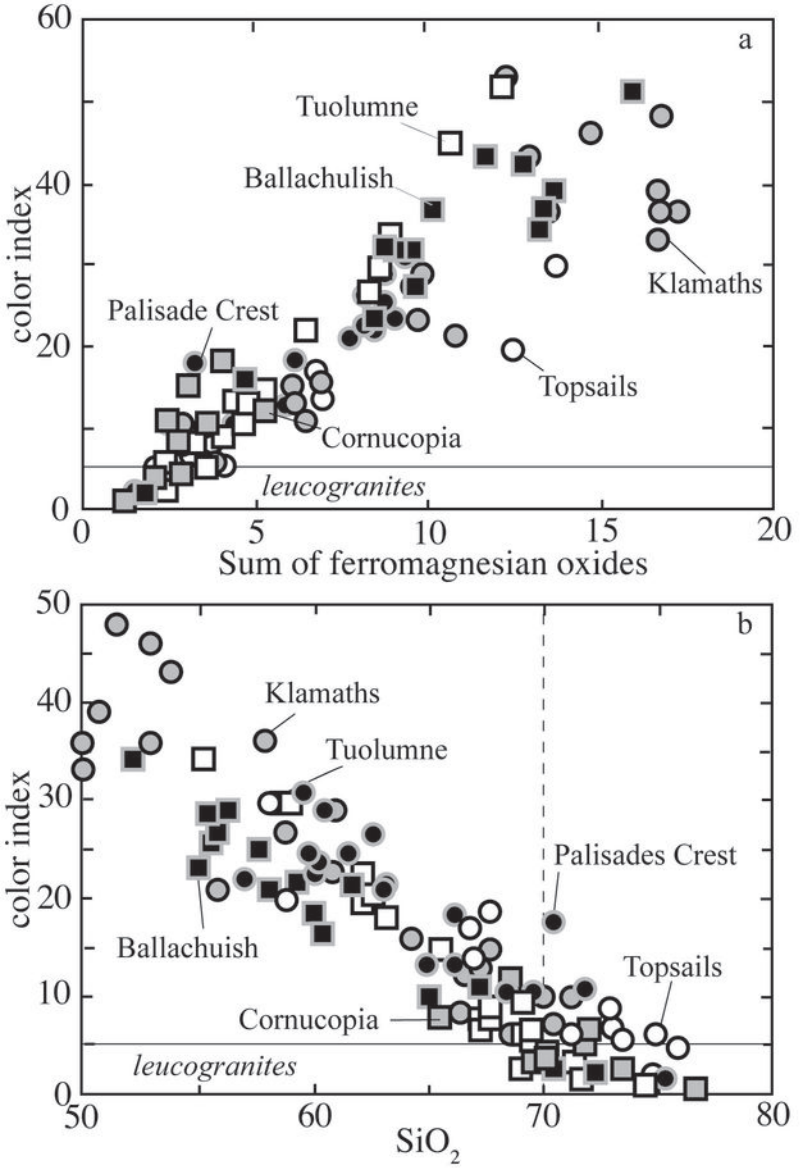

Frost et al., Fig. 1

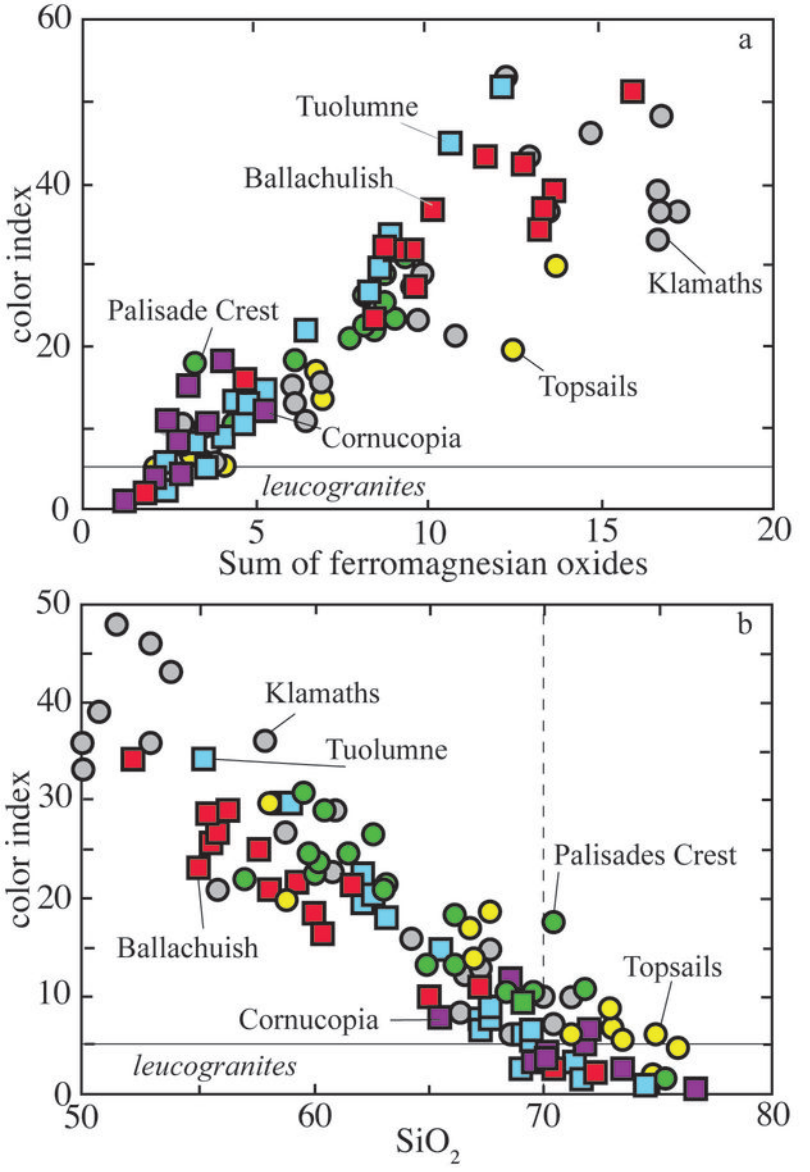

Frost et al., Fig. 1

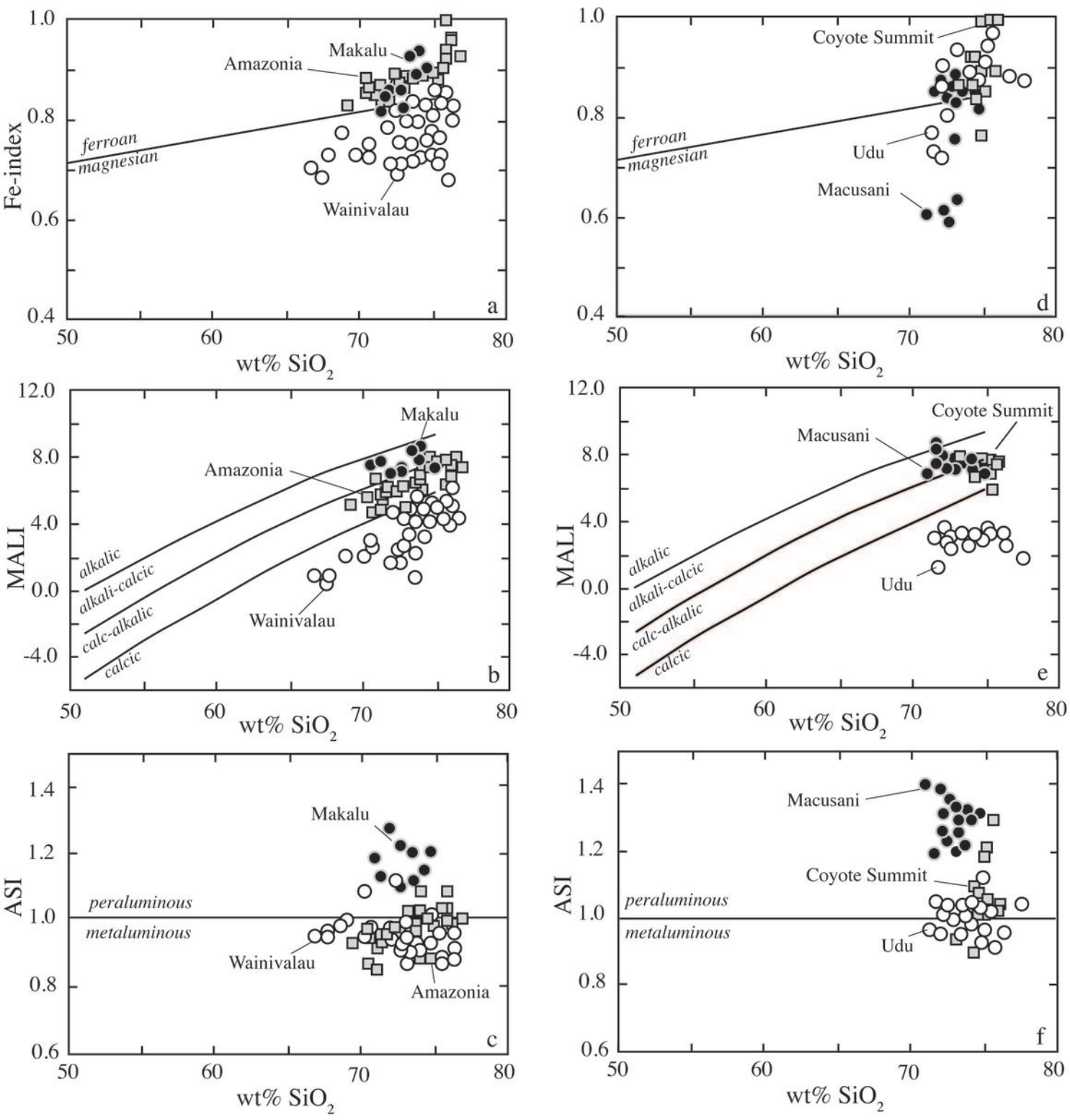

Frost et al., Fig. 2

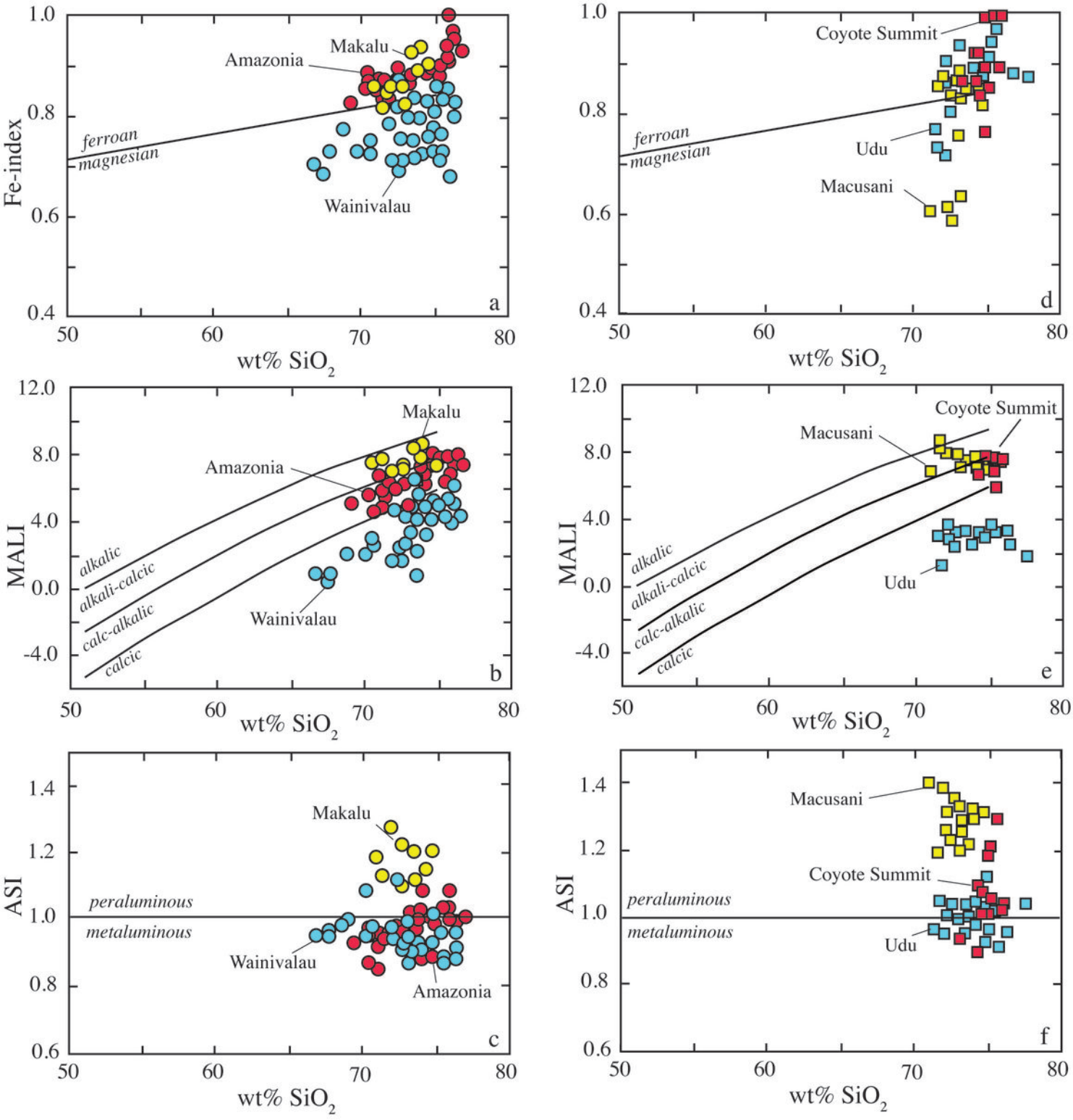

Frost et al., Fig. 2

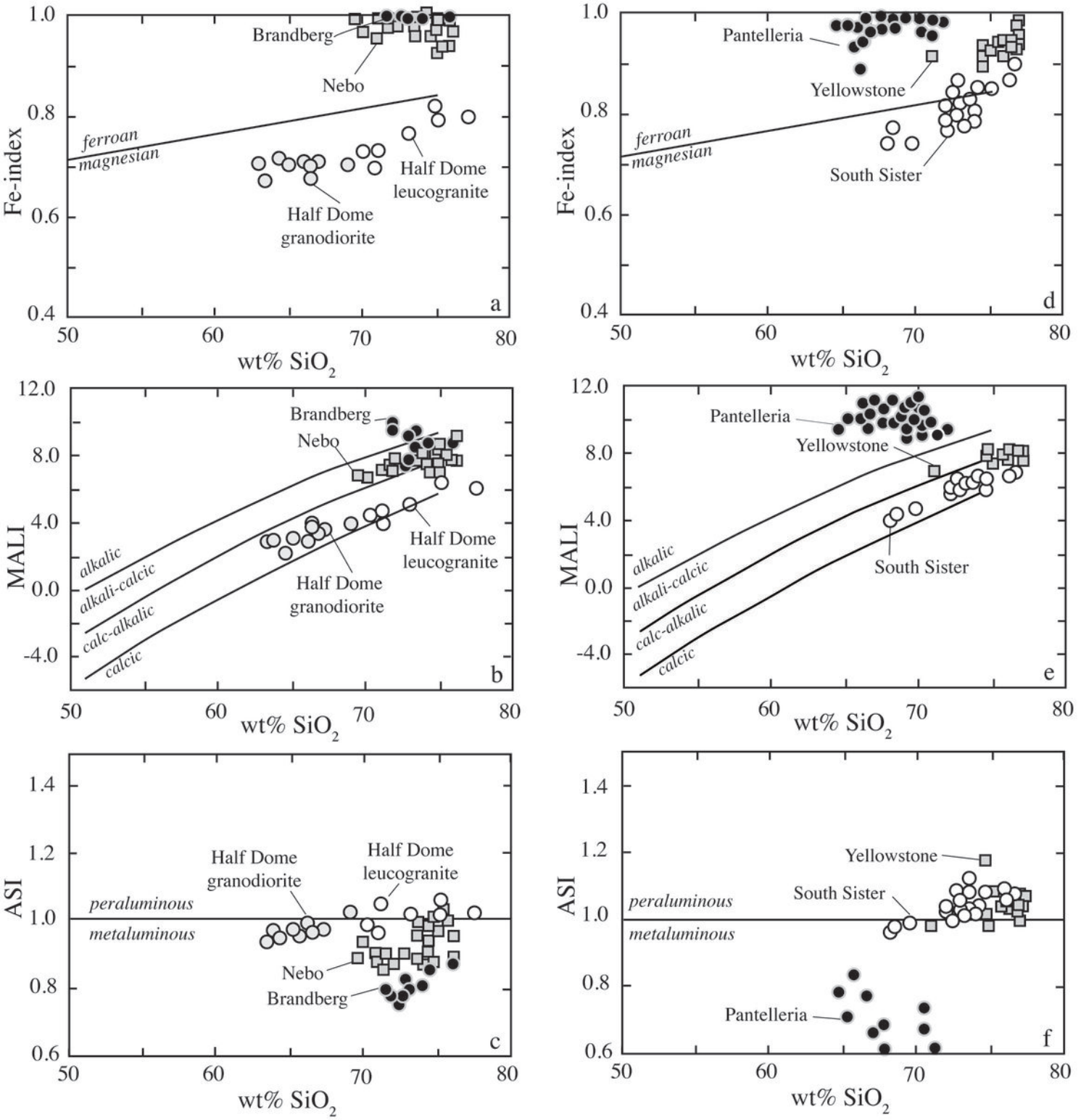

Frost et al., Fig. 3

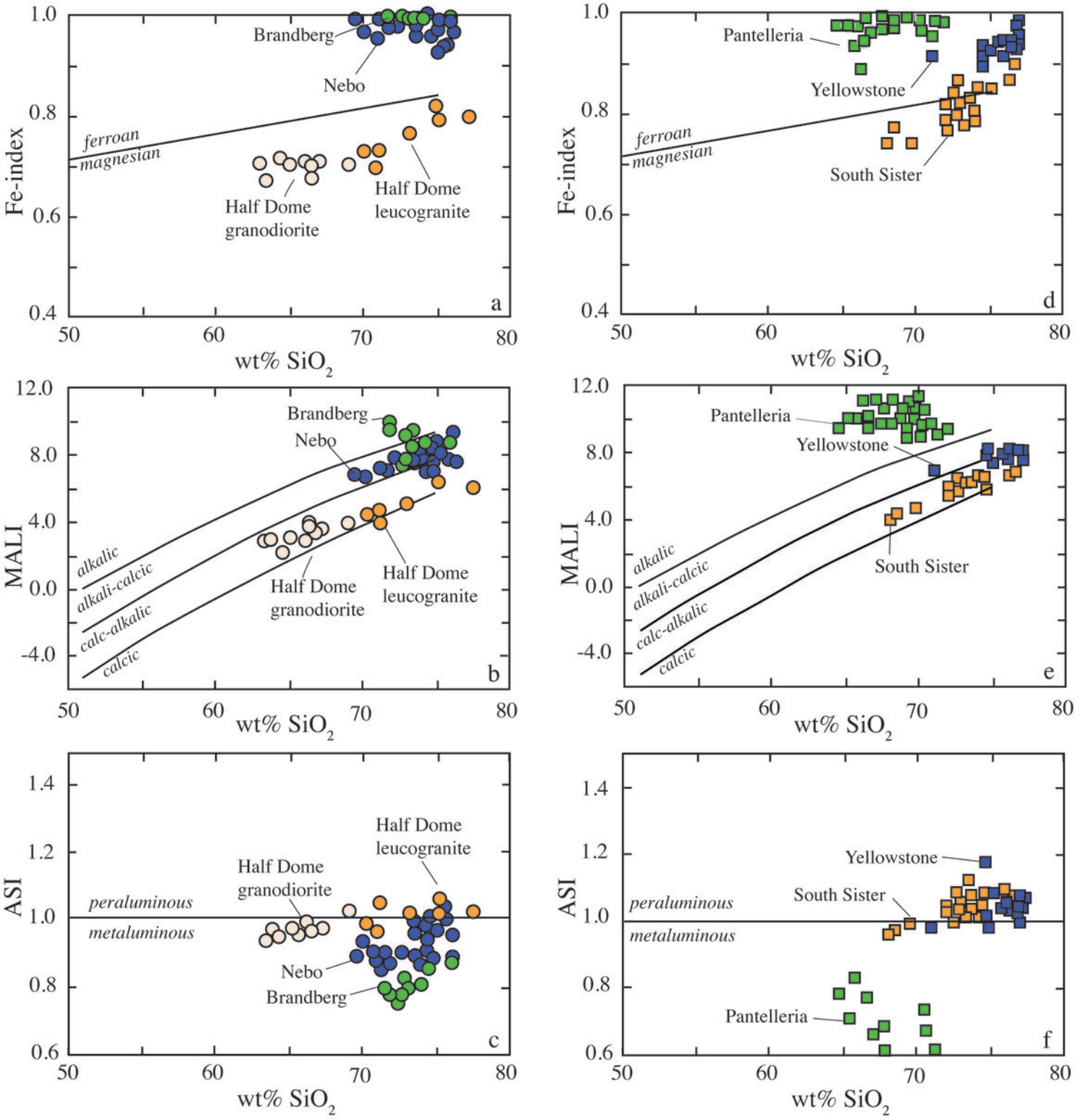

Frost et al., Fig. 3

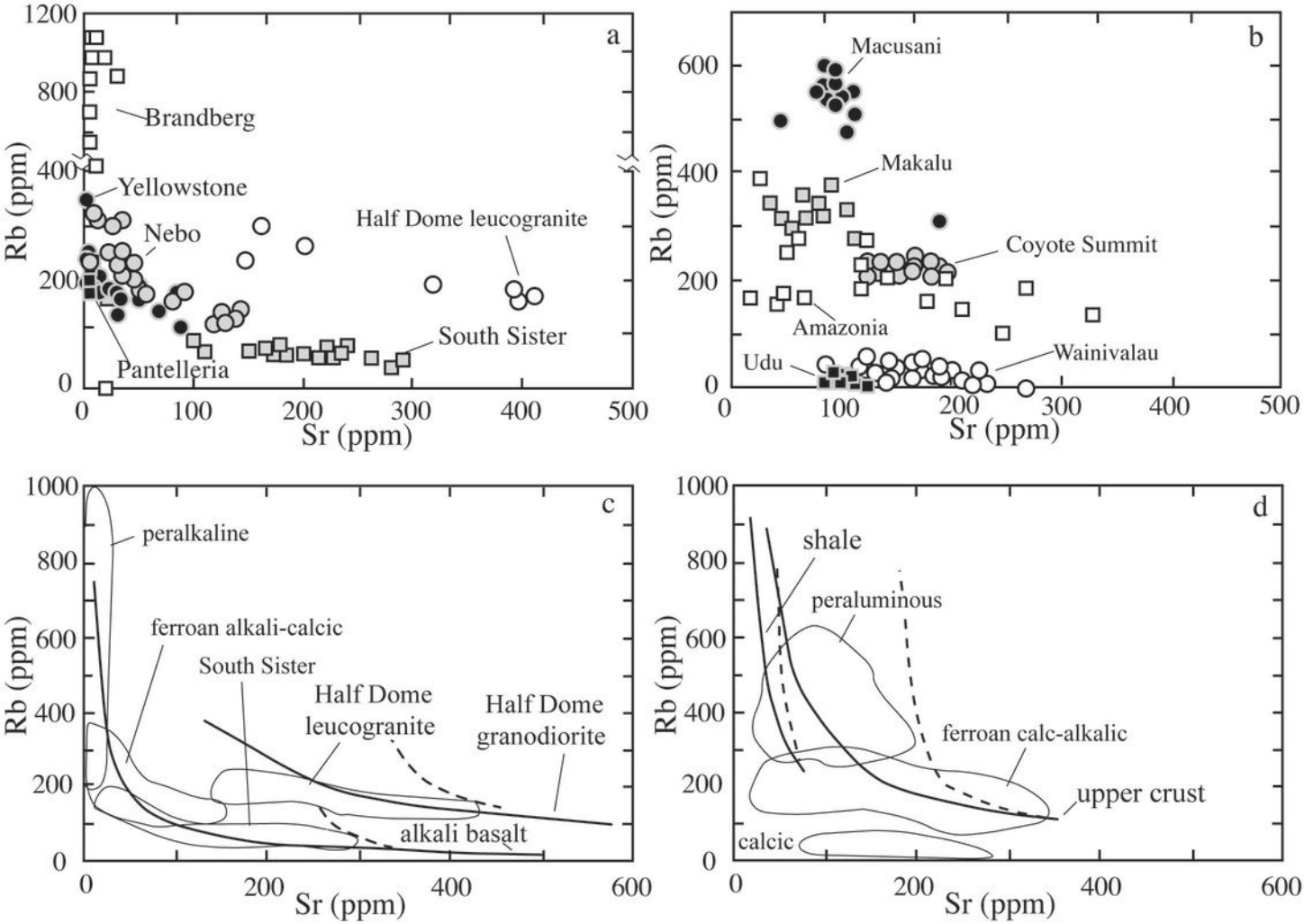

Frost et al., Fig. 4

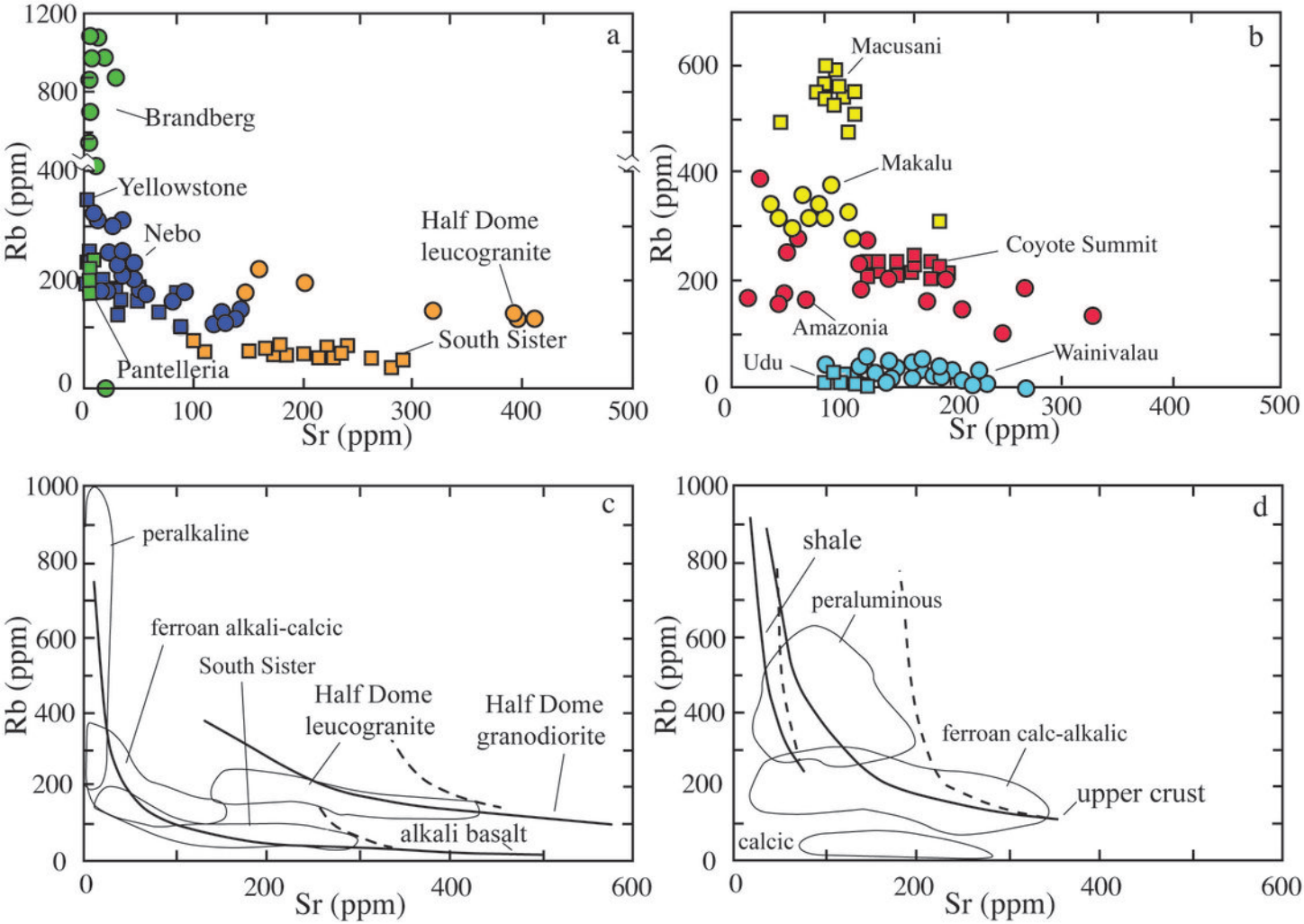

Frost et al., Fig. 4

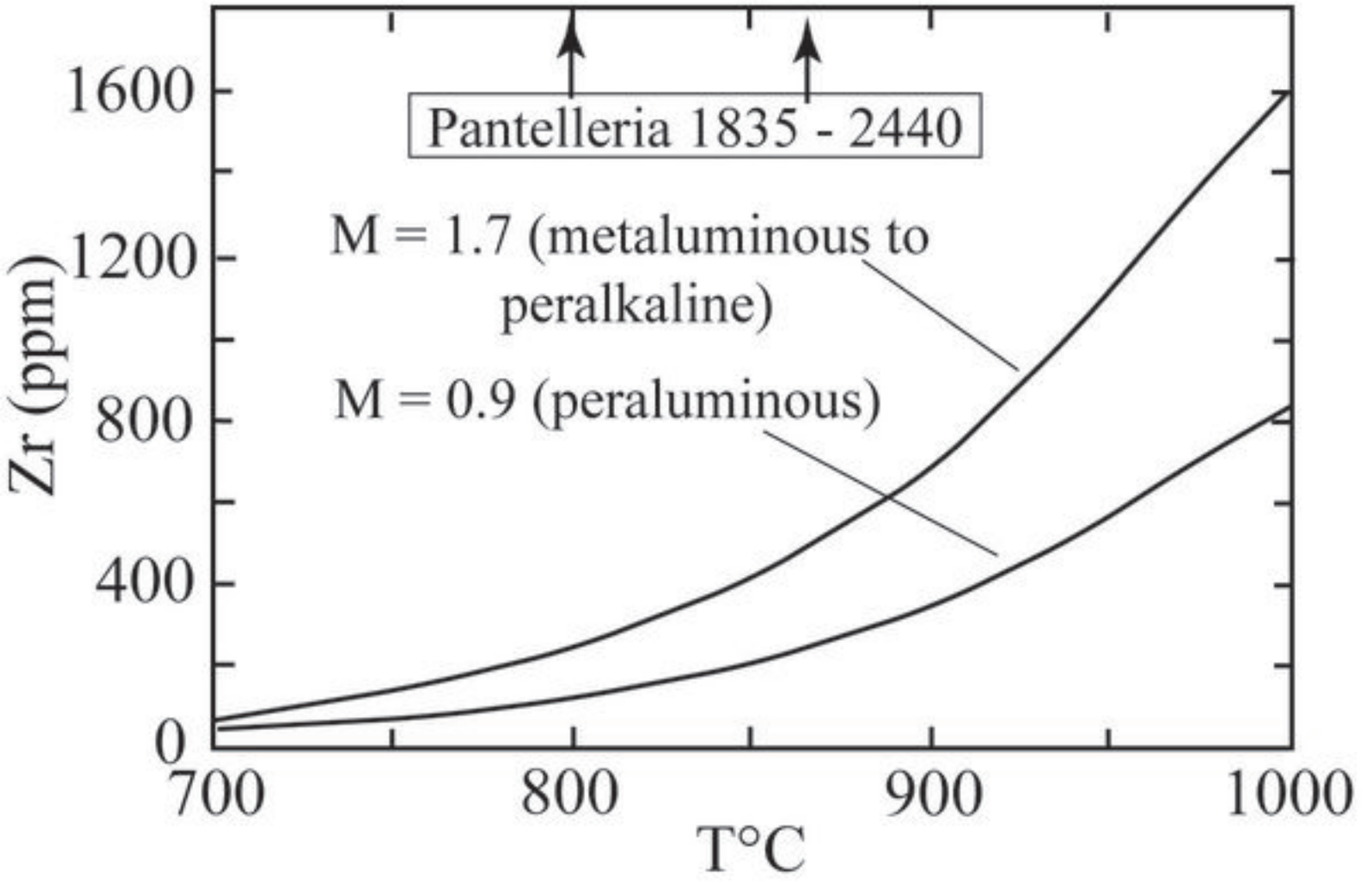

Frost et al., Fig. 5

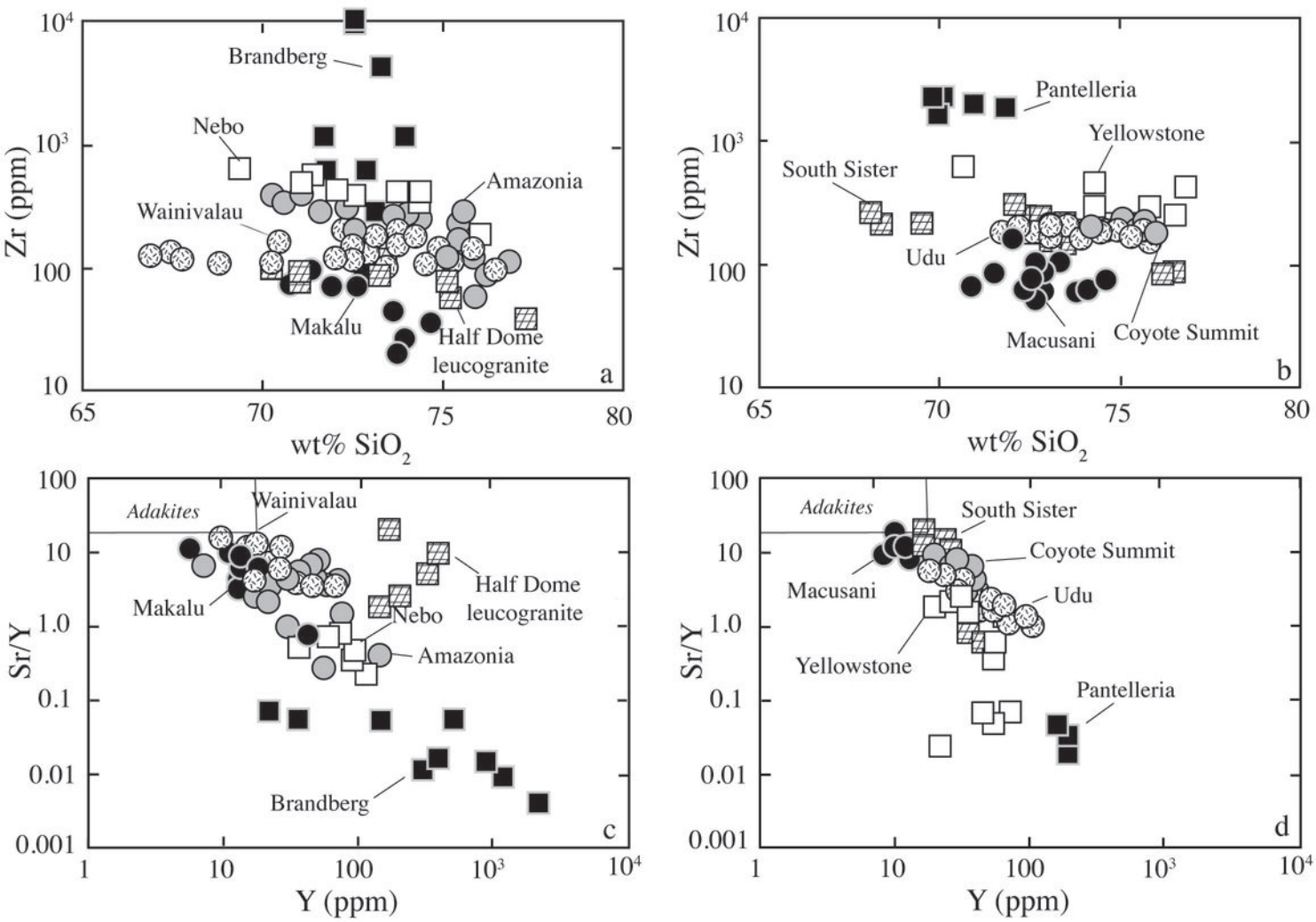

Frost et al., Fig. 6

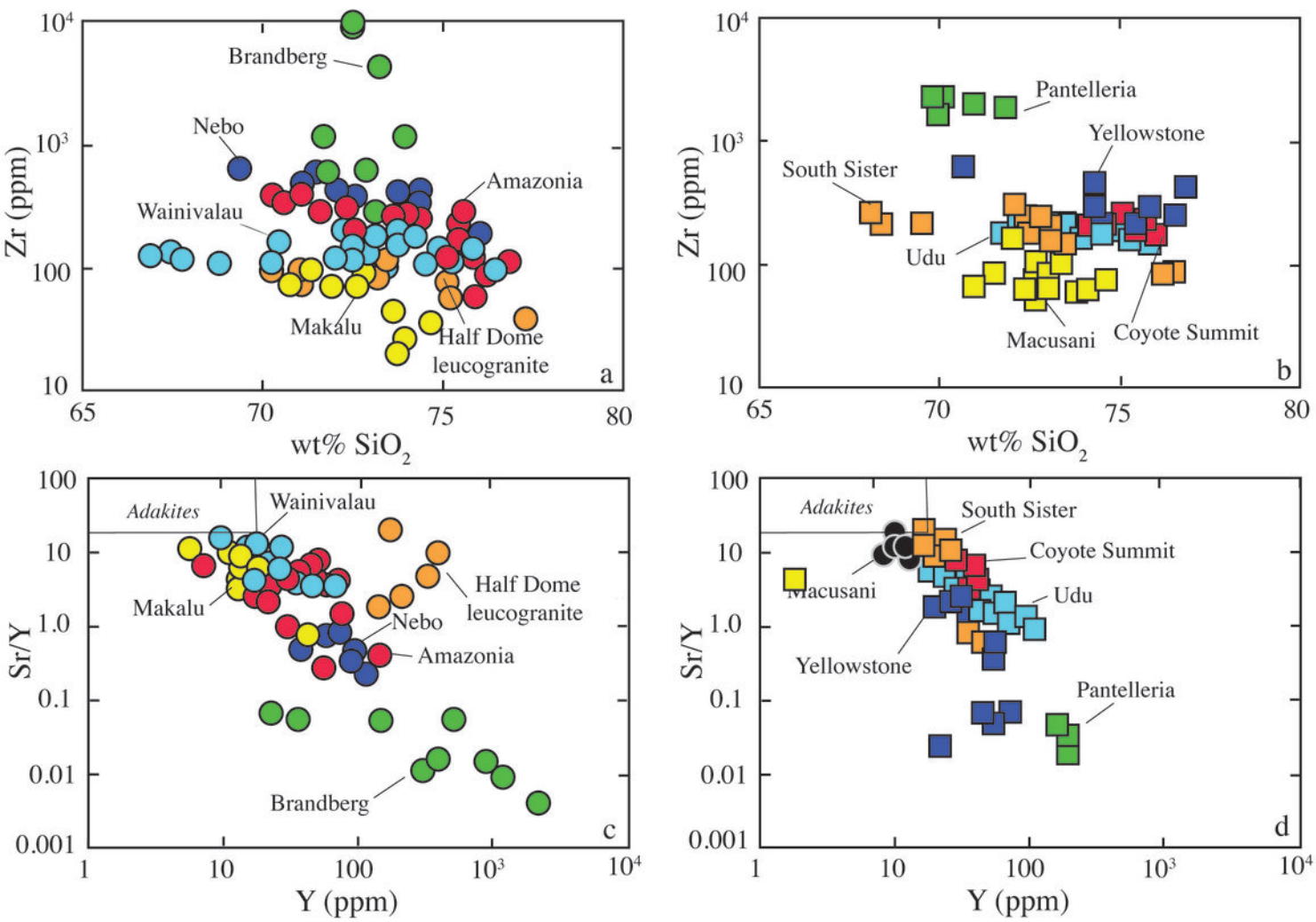

Frost et al., Fig. 6

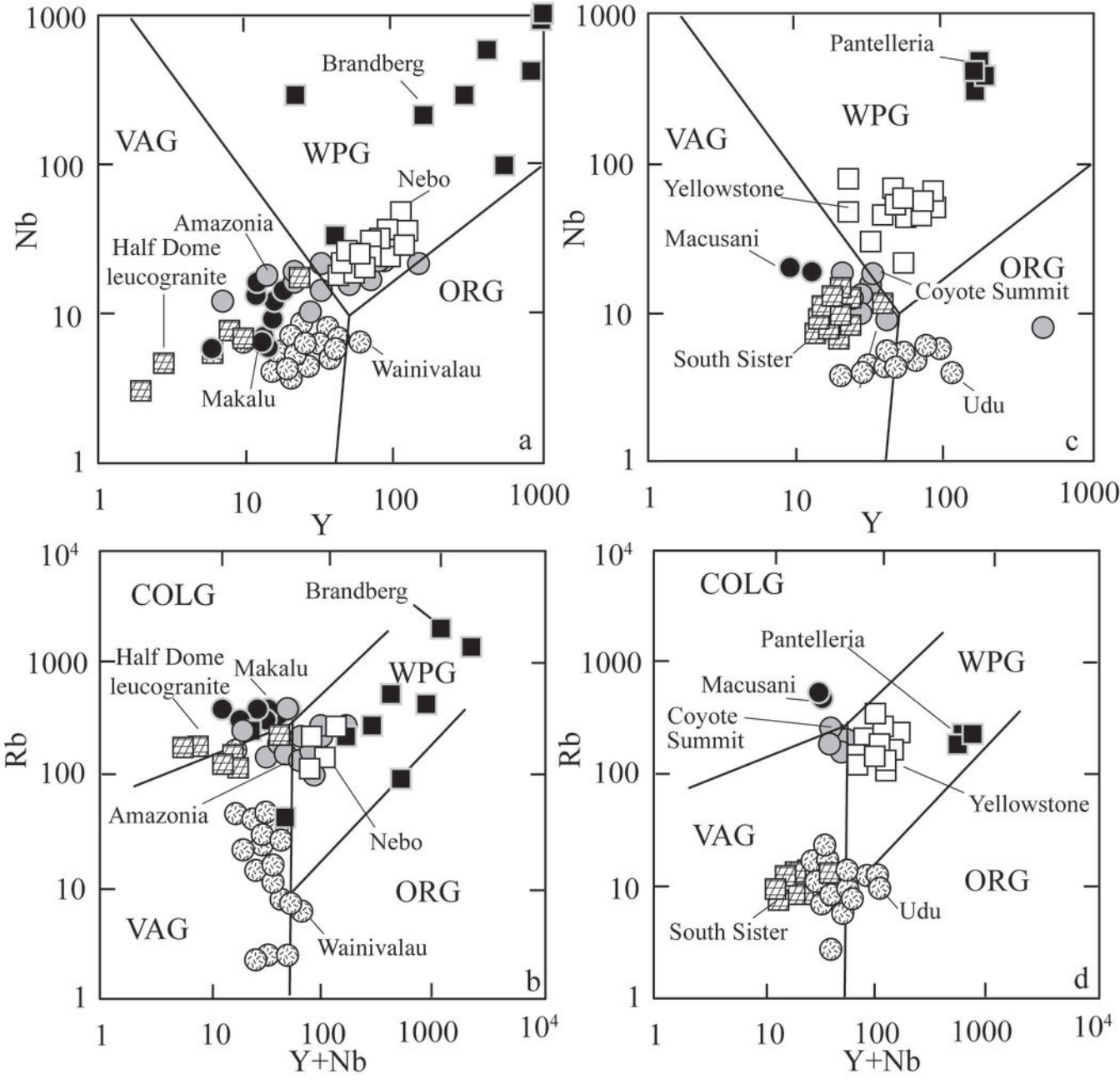

Frost et al. Fig. 7

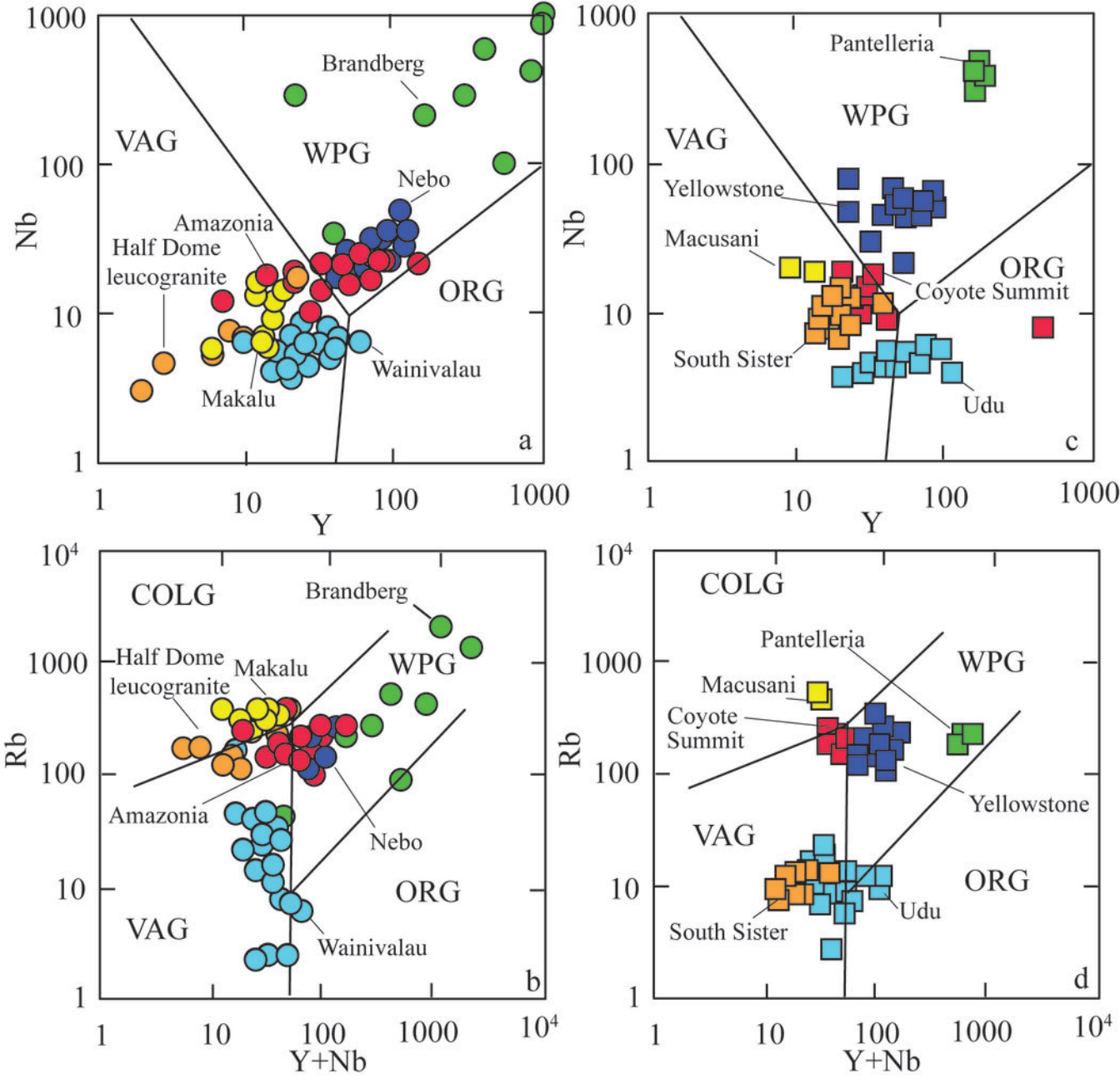

Frost et al. Fig. 7

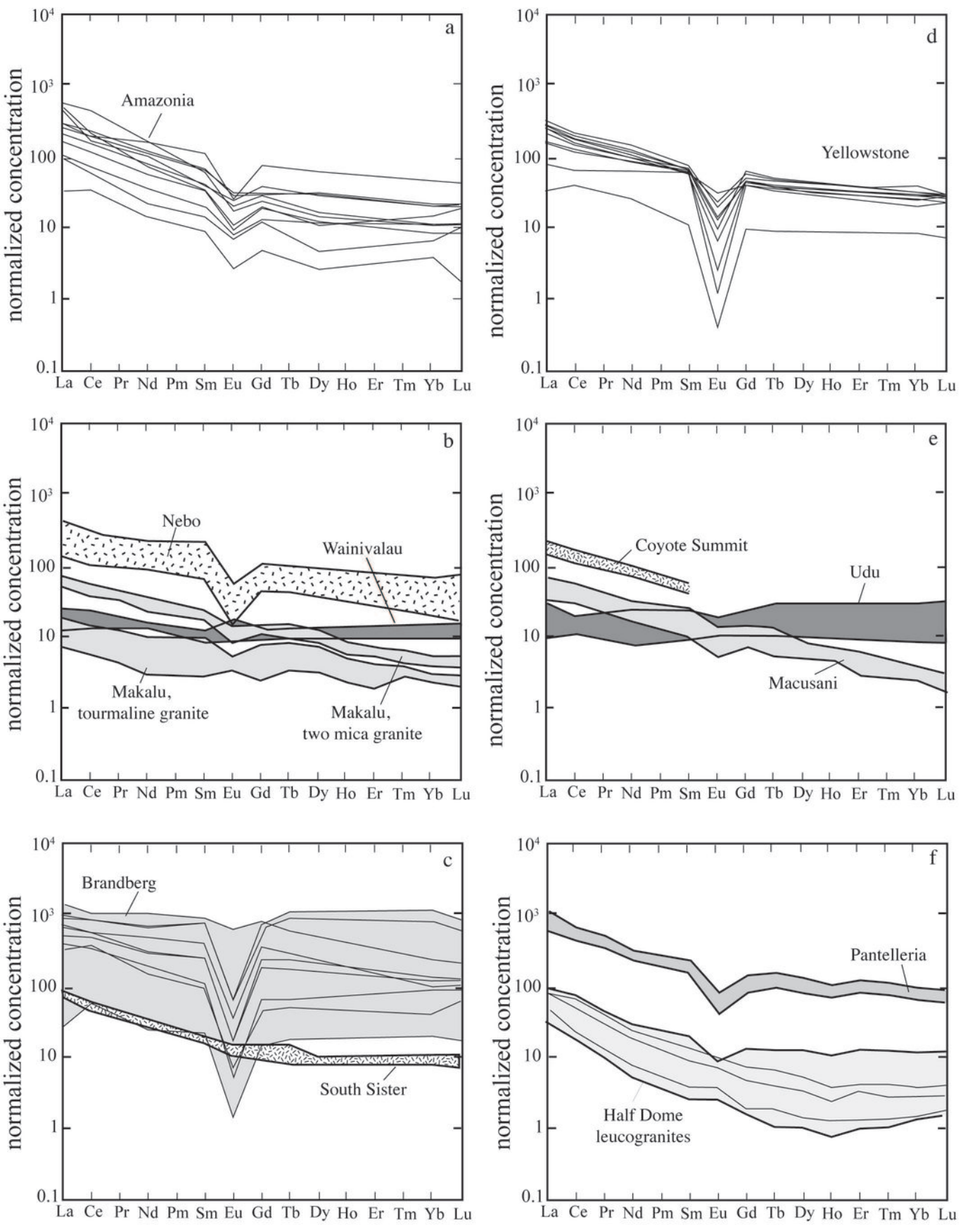

Frost et al. Fig. 8

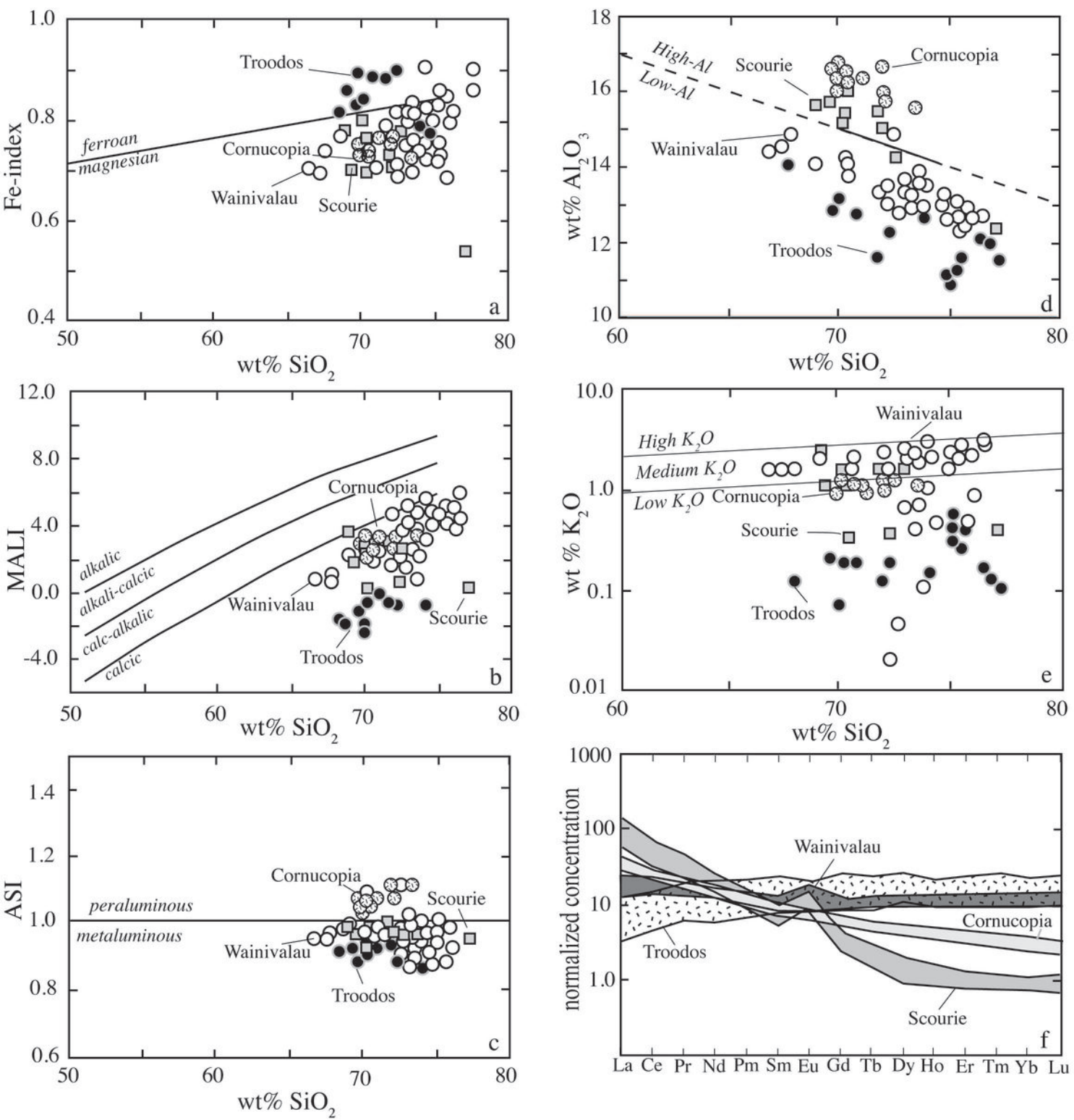

Frost et al., Fig. 9

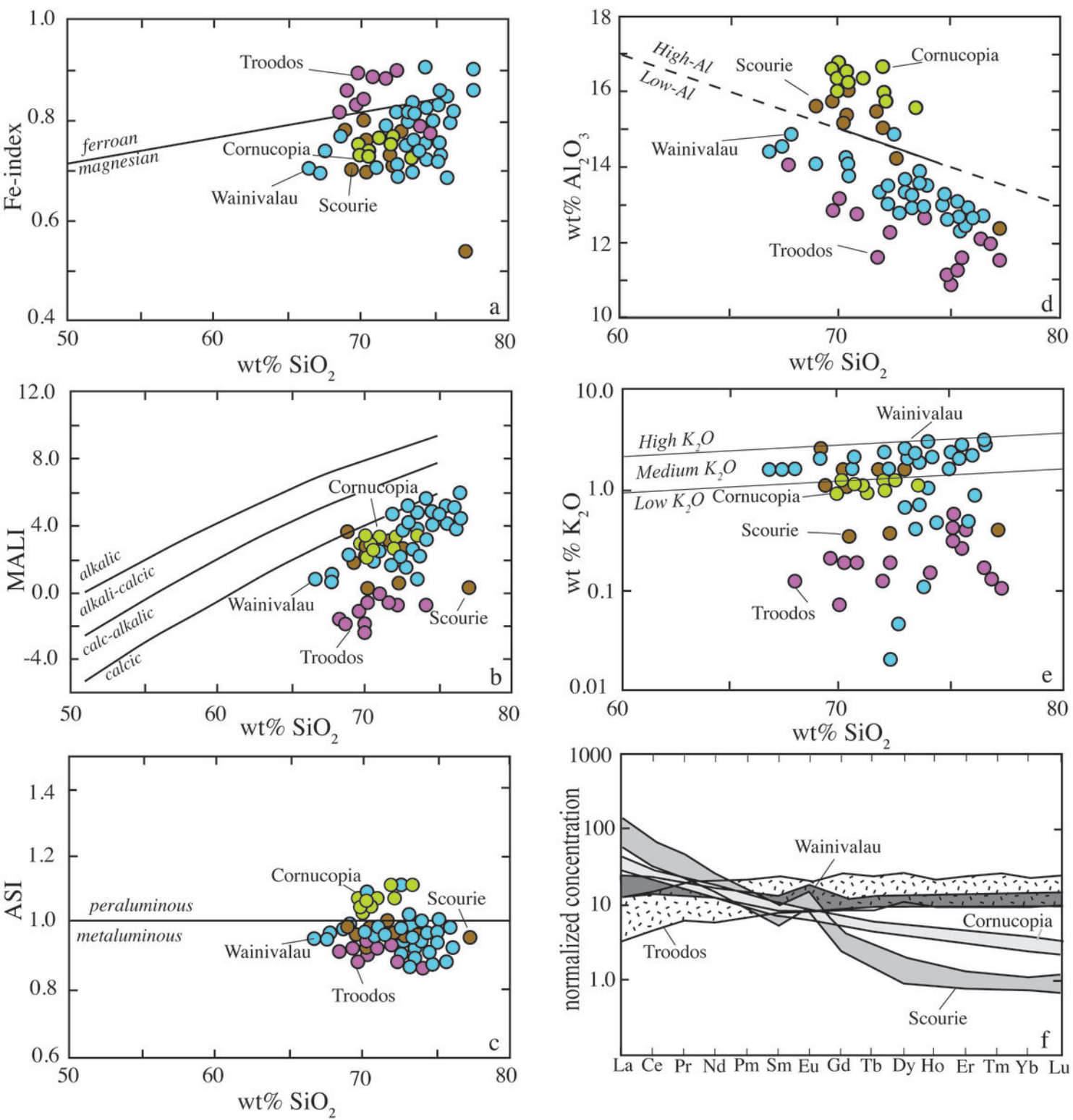

Frost et al., Fig. 9

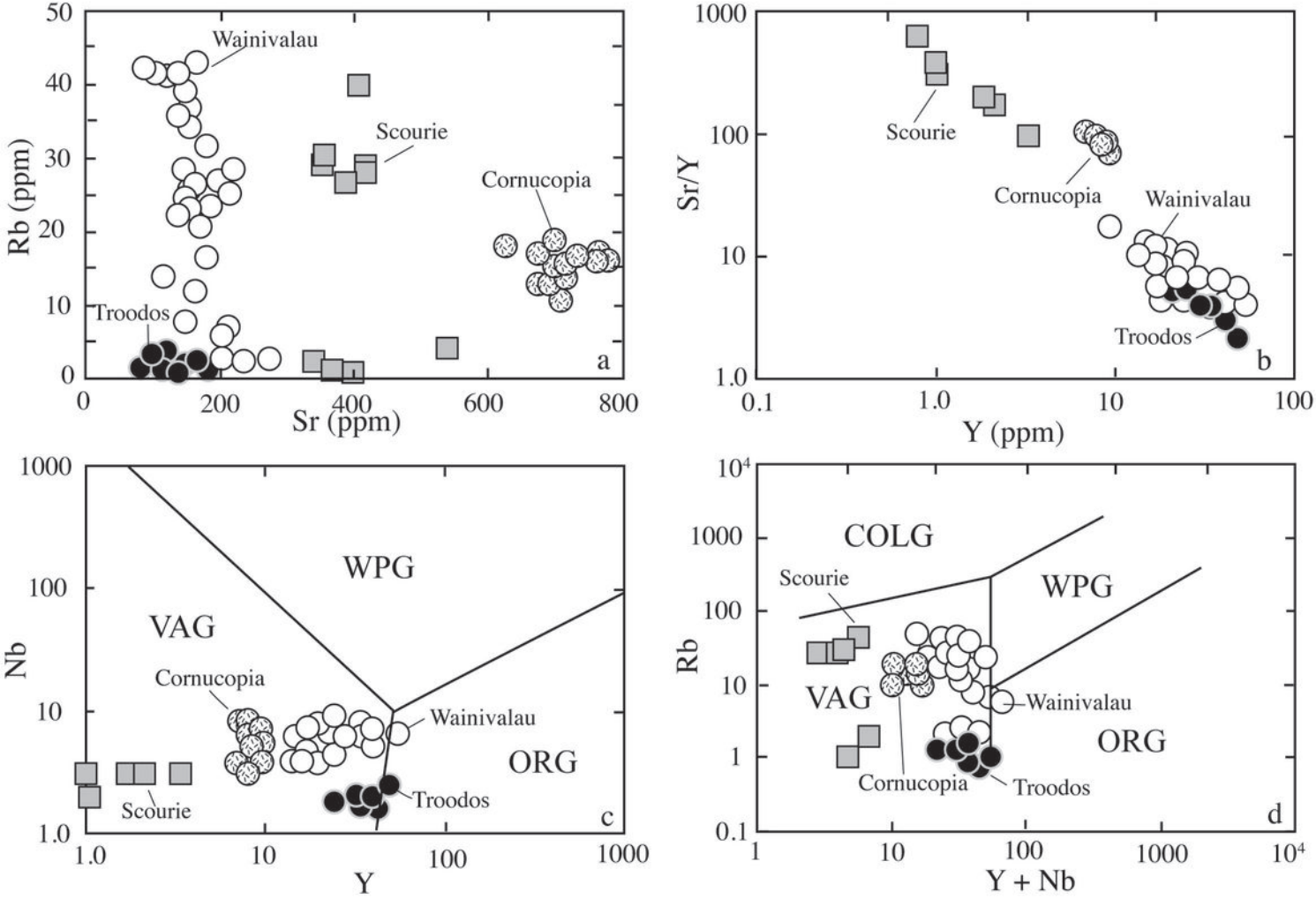

Frost et al., Fig. 10

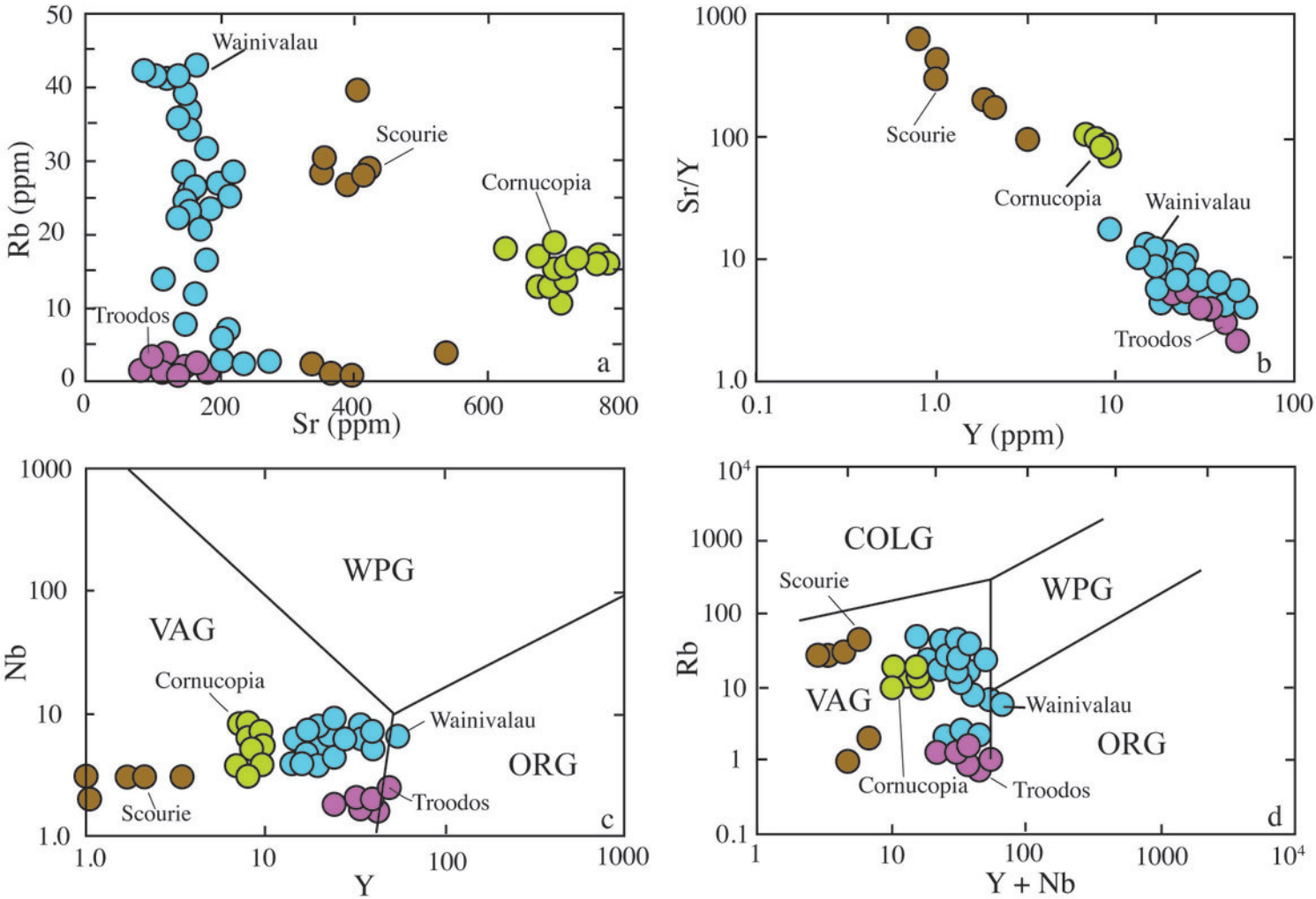

Frost et al., Fig. 10

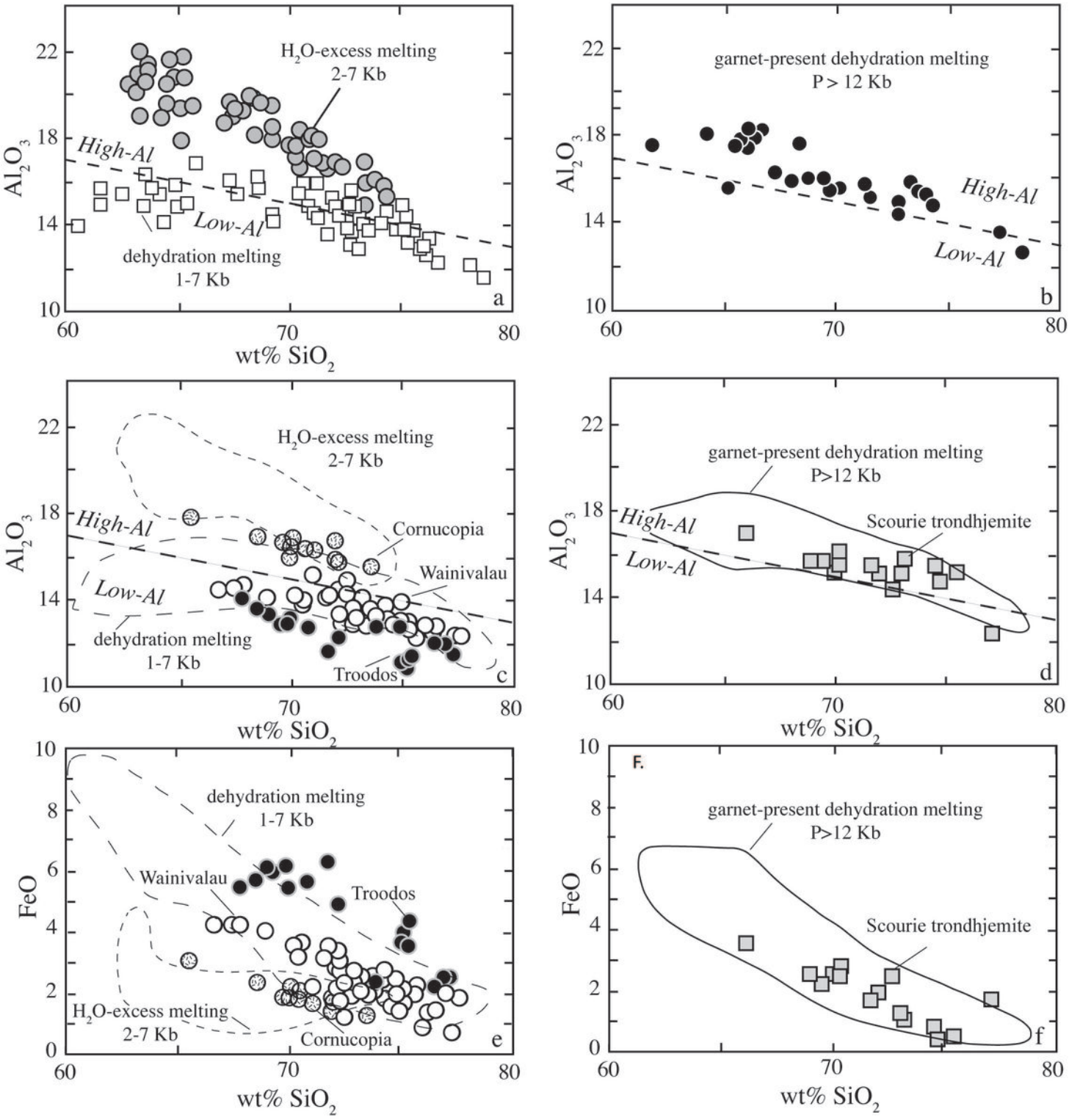

Frost et al., Fig. 11

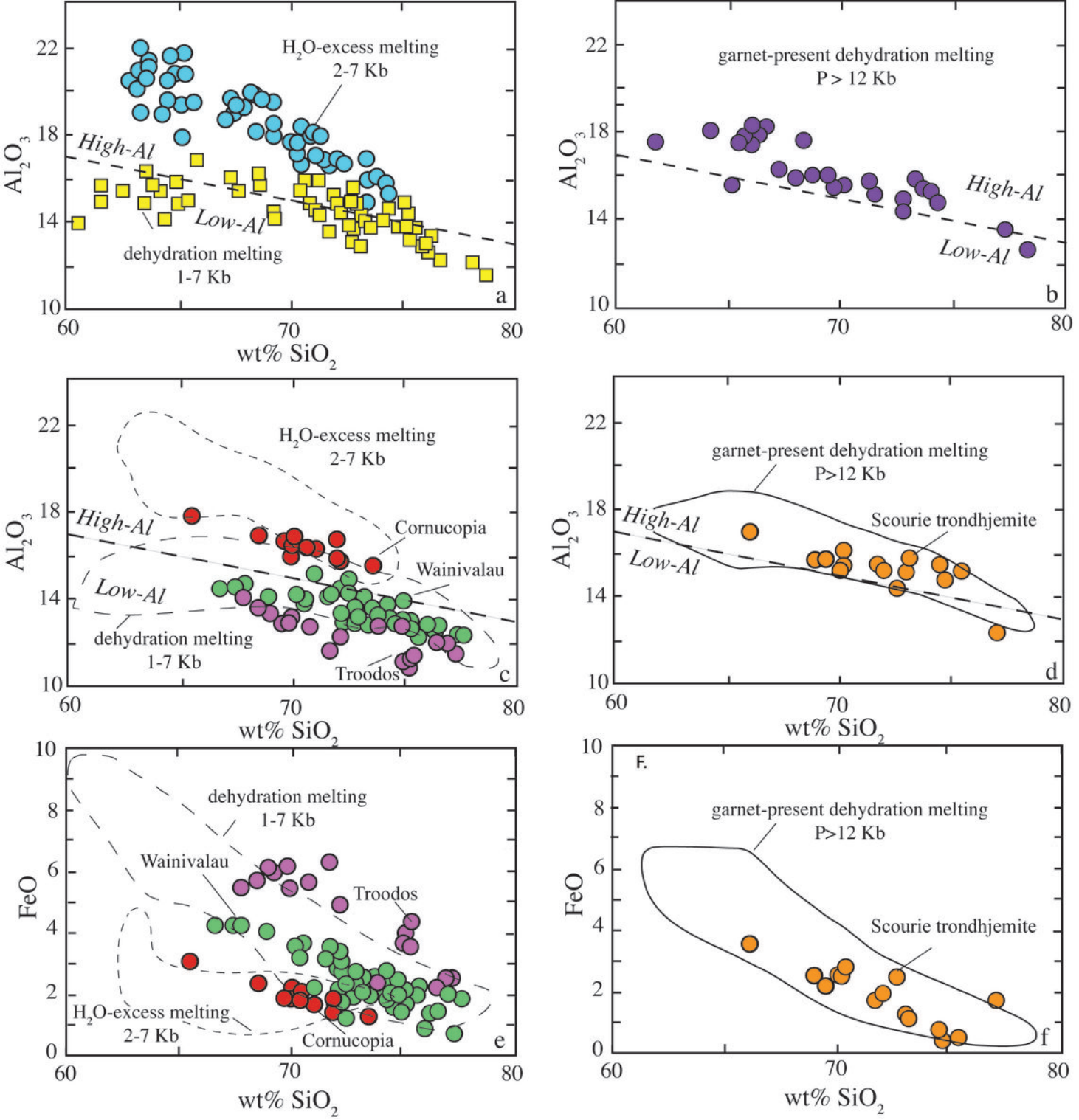

Frost et al., Fig. 11

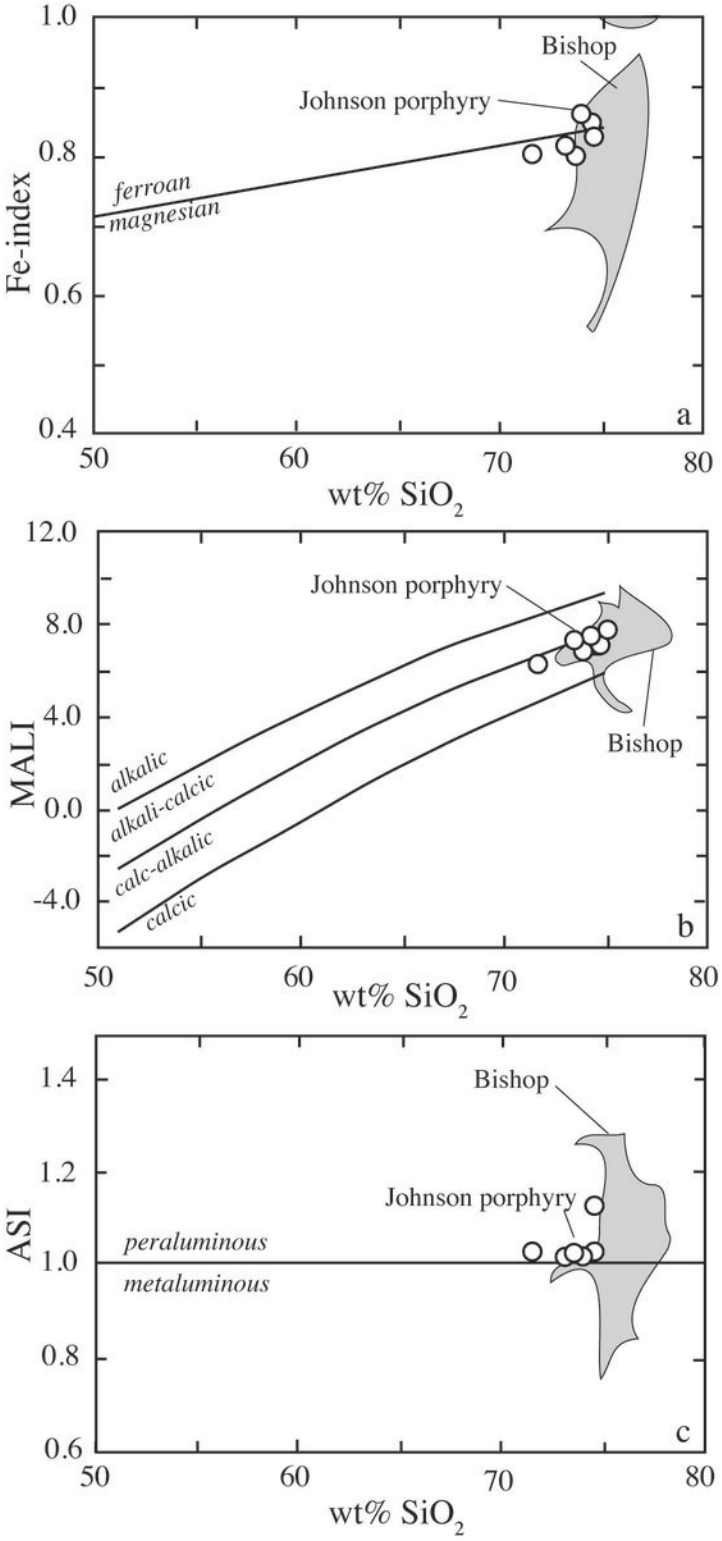

Frost et al., Fig. 12

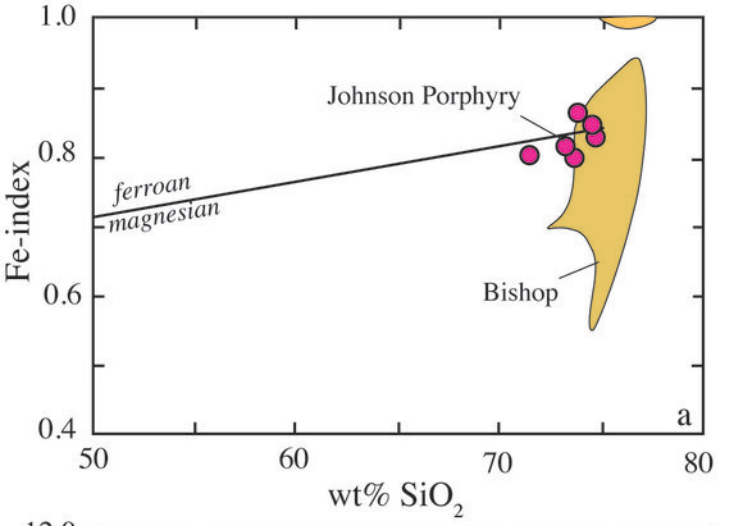

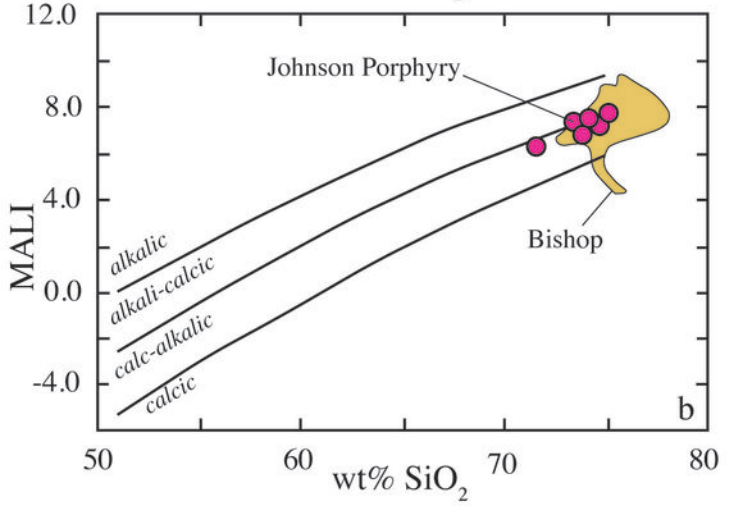

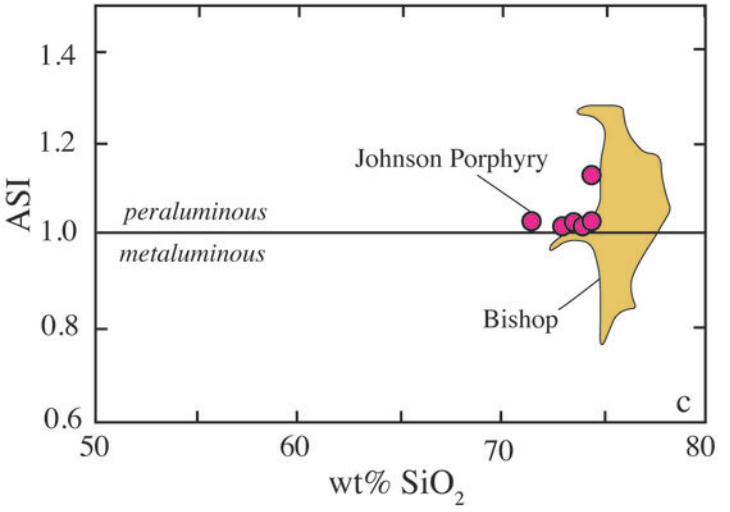

Frost et al., Fig. 12